AD-A048 191 CHARLES STARK DRAPER LAB INC CAMBRIDGE MASS F/G 13/8
NONDESTRUCTIBLE MESG PROGRAM.(U)
AUG 77 K TAYLOR
UNCLASSIFIED R-1089 AFAL-TR-77-159 F33615-74-C-1234 NL

1 OF 1
AD A048191

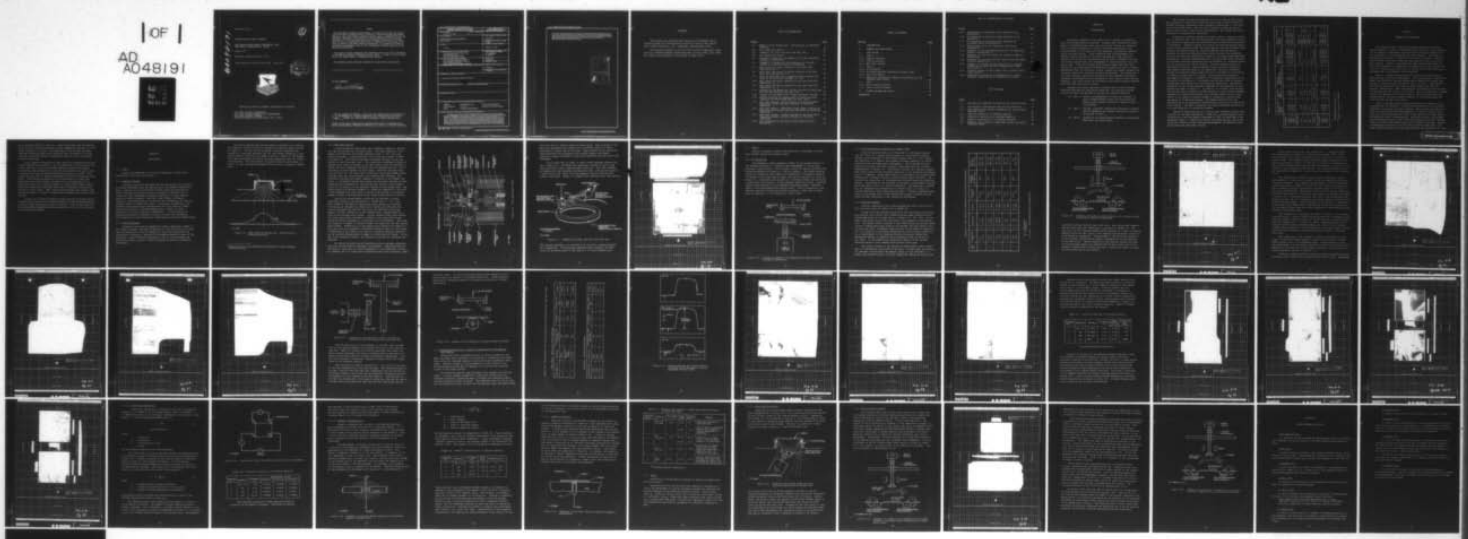

END
DATE FILMED
1-78
DDC

AD A048191

AFAL-TR-77-159

(1)

NONDESTRUCTIBLE MESG PROGRAM

The Charles Stark Draper Laboratory, Inc.
Cambridge, Massachusetts 02139

August 1977

TECHNICAL REPORT AFAL-TR-77-159

Final Report for Period July 1974 – June 1977

Approved for public release; distribution unlimited

AIR FORCE AVIONICS LABORATORY
AIR FORCE WRIGHT AERONAUTICAL LABORATORIES
AIR FORCE SYSTEMS COMMAND
WRIGHT-PATTERSON AIR FORCE BASE, OHIO 45433

NOTICE

When Government drawings, specifications, or other data are used for any purpose other than in connection with a definitely related Government procurement operation, the United States Government thereby incurs no responsibility nor any obligation whatsoever; and the fact that the government may have formulated, furnished, or in any way supplied the said drawings, specifications, or other data, is not to be regarded by implication or otherwise as in any manner licensing the holder or any other person or corporation, or conveying any rights or permission to manufacture, use, or sell any patented invention that may in any way be related thereto.

This report has been reviewed by the Information Office (OI) and is releasable to the National Technical Information Service (NTIS). At NTIS, it will be available to the general public, including foreign nations.

This technical report has been reviewed and is approved for publication.

_____ _____

FOR THE COMMANDER

Ronald J. Ringo

"If your address has changed, if you wish to be removed from our mailing list, or if the addressee is no longer employed by your organization please notify __RWA_____*,W-PAFB, OH 45433 to help us maintain a current mailing list".*

Copies of this report should not be returned unless return is required by security considerations, contractual obligations, or notice on a specific document.

SECURITY CLASSIFICATION OF THIS PAGE (When Data Entered)

REPORT DOCUMENTATION PAGE

READ INSTRUCTIONS BEFORE COMPLETING FORM

1. REPORT NUMBER: AFAL–TR–77-159	2. GOVT ACCESSION NO.
3. RECIPIENT'S CATALOG NUMBER	
4. TITLE (and Subtitle): NONDESTRUCTIBLE MESG PROGRAM FINAL REPORT	5. TYPE OF REPORT & PERIOD COVERED: Final Report
6. PERFORMING ORG. REPORT NUMBER: R-1089	
7. AUTHOR(s): K. Taylor	8. CONTRACT OR GRANT NUMBER(s): F33615-74-C-1234
9. PERFORMING ORGANIZATION NAME AND ADDRESS: The Charles Stark Draper Laboratory, Inc. 555 Technology Square Cambridge, Massachusetts 02139	10. PROGRAM ELEMENT, PROJECT, TASK AREA & WORK UNIT NUMBERS: FY11757400480 01, 02/666A
11. CONTROLLING OFFICE NAME AND ADDRESS: Air Force Avionics Laboratory (RWA) Air Force Wright Aeronautical Laboratories Air Force Systems Command Wright-Patterson Air Force Base, Ohio 45433	12. REPORT DATE: August 1977 13. NUMBER OF PAGES
14. MONITORING AGENCY NAME & ADDRESS(if different from Controlling Office)	15. SECURITY CLASS. (of this report): Unclassified 15a. DECLASSIFICATION/DOWNGRADING SCHEDULE

16. DISTRIBUTION STATEMENT (of this Report)

Approved for public release; distribution unlimited.

17. DISTRIBUTION STATEMENT (of the abstr[illegible]ed in Block 20, if different from Report)

18. SUPPLEMENTARY NOTES

19. KEY WORDS (Continue on reverse side if necessary and identify by block number)

MICRON	High Speed Wear Test	Titanium Carbide Deposition
Sputter Deposition	Thin Films	Molybdenum Disulphide Deposition
MESG	Tungsten Carbide Deposition	

20. ABSTRACT (Continue on reverse side if necessary and identify by block number)

A program was carried out to develop suitable surface hard-coatings to render MESG bearing hardware indestructible. A test program to determine friction and wear characteristics of carbide-type materials in the MESG environments was carried out and a carboloy-type coating of WC+Co was selected for the final cavity surface and a thin film of molybdenum sulfide was selected for the rotor surface. Tests were also carried out to determine other coating properties such as magnetic susceptibility, electrical resistivity and adhesion. Suitable coating procedures based on vacuum deposition techniques such as sputtering and electron beam evaporation were also developed and successfully used to coat both specimens for tests and final MESG cavity and rotor parts. A total of eight MESG

DD FORM 1 JAN 73 1473 EDITION OF 1 NOV 65 IS OBSOLETE

SECURITY CLASSIFICATION OF THIS PAGE (When Data Entered)

rotors were successfully coated with molybdenum disulfide approximately 0.20 μm thick and six sets of cavity parts were coated with an intermediate layer of Inconel by substrate biased high-rate-electron beam evaporation (ion-plated) and a final layer of WC+Co by hollow cathode-type planar magnetron sputtering. These parts were then delivered to the Autonetics division of Rockwell International Corporation for testing.

FOREWARD

This report was prepared under Project FY11757400480, AMD 01, 02/666A through Air Force Contract F33615-74-C-1234 by The Charles Stark Draper Laboratory, Inc., Cambridge, Massachusetts 02139.

The sponsoring agency is the Air Force Avionics Laboratory (RWA), Air Force Systems Command, Wright-Patterson Air Force Base, Ohio 45433. This report was submitted by the author in August 1977.

LIST OF ILLUSTRATIONS

TABLE OF CONTENTS

LIST OF TABLES

SECTION 1

INTRODUCTION

The primary emphasis of the effort was to develop a nondestructible micro-electrostatic gyroscope. Program tasks included the development of nondestructible rotor and cavity sets; conduct an investigation of micron performance in various potential applications; and perform studies in the areas of micron modeling, calibration, mechanization and test results. Tasks concerned with the development of a complete familiarization of the micron program and other potential applications for micron were discontinued by AFAL in December 1974 and activities centered about the development of nondestructible rotor and cavity sets. This work defined three separate tasks with the first calling for an investigation of materials to permit the gyro to restart immediately after an electronic failure induced high speed touchdown and to remain operational following system recalibration. The second was a fall-back position, permitting the reuse of the components following touchdown, disassembly and the relapping of rotor and/or cavity bearing surfaces. The third called for the reuse of the gyro following replacement of either the rotor or cavity.

Because the efforts required to perform each of the previously described subtasks are essentially identical, the following revised subtask division was designed to achieve the required objective.

(1) Task 1: Design and development of fixturing necessary to obtain nondestructible rotor and cavity parts by applying hard surface coatings to spherical bearing surfaces.

(2) Task 2: Coating, finishing, testing and evaluation of specimens to determine the optimum coating and finish to be applied in Task 3.

(3) Task 3: Evaluation of coated bearing surfaces on operational MESG rotor and cavity parts.

The original program required CSDL to coat 12 sets of MESG rotors and housings (12 rotors and 24 housing halves) and to assist Strategic Systems Division, Autonetics Group, Rockwell International in the analysis of the tested parts, The Air Force changed the scope of the program to coat 6 sets of MESG rotors and housings. The coated parts were delivered to Autonetics for evaluation.

Coatings of tungsten carbide with cobalt (WC+Co), tungsten carbide with no additive (WC). and titanium carbide (TiC) were selected as possible choices for deposition onto beryllium and beryllium oxide substrates by sputtering. Tungsten carbide with cobalt was selected because experience on other programs showed that solid bearing parts manufactured from carboloy 44A (WC+6 percent Co) gave long bearing life and sputter deposits on beryllium substrates from carboloy targets gave excellent friction and wear test results when tested in the normal gyroscope wheel environment. Titanium carbide deposited onto beryllium oxide substrates by activated reactive evaporation was also selected as a possible choice for the coating on the cavity surface. Titanium carbide coatings of sufficient thickness to satisfy surface finish and other dimensional requirements have been shown by low speed wear testing to withstand periods of sustained rubbing under load with no evidence of wear debris or change in coefficient of friction. This process was originally developed by Professor R.F. Bunshah[1] of the Materials Department of the University of California at Los Angeles and has been shown to produce consistently hard deposits on flat beryllium substrates. Engineering properties of the coating materials selected for consideration in this program are shown in Table 1-1. In addition to carbides, both borides and nitrides were considered, borides because of their extreme hardness compared to nitrides and carbides, and nitrides because of the simple nature of the chemical reaction needed to accomplish a reactive-type sputtering or evaporation process. Molybdenum disulfide was also considered to be an acceptable lubricant-type coating for the beryllium rotor surface. The work of Spalvins[2] has shown molybdenum disulfide to be a good lubricant in vacuum environments.

Series of tests were set up to insure that selected coatings were suitable for the MESG application. These tests included magnetic susceptibility by the Gouy Method (developed in 1889) as described in NBS monograph number 4[3], adhesion by tensile pull-type testing, electrical resistivity based on sheet resistance measurements and abrasion resistance using high speed wear testing.

Table 1-1. Engineering properties of materials for hard coatings.

	Theoretical Density gm/cc	Specific Heat BTU/lb/^{o}F	Thermal Conductivity BTU/(hr)(ft)(^{o}F)	Thermal Expansion 10^{-6} in./in./^{o}F	Micro Hardness Knoop KG/mm^{2}
Borides					
TiB_2	4.52	0.15	40	4.8 (70-4000)*	3000 (100** gm)
ZrB_2	6.09	0.10	48	4.6 (70-4000)*	2100 (160)
HfB_2	11.20	0.07	30	4.2 (70-4000)	2400 (160)
Carbides					
TiC	4.92	0.12	18	40 (70-1500)	2000 2700 (50)
TcC	14.50	0.04	—	3.7	1800 2400 (30, 100)
WC	15.8	0.04	—	2.9	1700 2400 (50)
WC+Co	11–15.2	0.03–0.06	16—30	3.0 6.0 (70-1800)	1100
Nitrides					
TiN	5.44	0.14	12	4.5 (70-1100)	1800 (100)
TcN	14.36	0.05	6.0	2.0 (70-1300)	1060 (50)
ZrN	7.35	0.09	5.5	3.9 (70-1100)	1500 (100)

*Temperature limits in ^{o}F

**Load in grams on indenter

SECTION 2

SUMMARY AND CONCLUSIONS

Test program results show that tungsten-carbide and titanium-carbide deposits as used in instrument applications can satisfy electrical and magnetic requirements when sufficient thickness necessary for the achievement of bulk properties has been achieved. The effect of thickness with respect to electrical resistivity is shown in the test results where the thinner films are more resistive than the thicker bulk deposits. Magnetic susceptibility tests showed that these carbides are nonmagnetic as deposited, and adhesion tests have shown that a level of bond strength sufficient to satisfy most of the fabrication and operational requirements can be achieved.

Wear is a surface deterioration of contacting surfaces which destroys their operating relationship. The brief period of testing has shown that significant surface deterioration takes place through the tearing of particles from the surface due to friction. The potential for surface seizure was also shown to exist between the selected material combinations. Wear from adhesion is indicated by the transfer of material from one surface to the other. Wear from abrasion is suggested by the character of the wear tracks in the softer beryllium substrates and by the nearly complete removal of the sputter deposited coatings from the wear track areas.

Some of the many factors affecting friction are surface finish, contamination, and hardness. Surface finish defines the size and distribution of the areas of actual contact. This testing has shown the need for high quality surface preparation in order to minimize high spots and local asperities that lead to the generation of wear debris and potential thin film penetration. Deep wear tracks in the coated beryllium substrates may result from the break-up of the thin carbide film as the hard film particles act as an abrasive substance. Surface contamination consisting of a thin film of oxide, water vapor, and other adsorbed impurities occurs when surfaces are cleaned in air, and

has a profound effect on friction. Others have shown that the removal of this film by vacuum outgassing at high temperature results in a very large increase in friction. The magnitude of the friction and wear observed throughout these tests indicates that the addition of solid lubricant-type films would be potentially beneficial as a controlled surface contaminant.

After complete evaluation of test results and experience with the various deposition processes it was concluded that the best choice for a wear resistant coating on the MESG bearing surfaces was tungsten carbide with cobalt deposited on the beryllium oxide cavity part using a magnetically-assisted hollow-cathode-type deposition system. This system was also used to deposit molybdenum disulfide on beryllium rotor parts. Difficulties encountered in the preparation of a pore free beryllium oxide cavity surface resulted in the consideration of an interfacial layer that could be lapped to a dense defect-free surface. High rate evaporation techniques were used to evaporate titanium and Inconel on cavity parts. Best results were obtained with Inconel coatings with respect to control of deposition parameters and ease of final lapping.

A total of six sets of beryllium oxide cavities were delivered to Autonetics for testing with tungsten carbide with cobalt deposited onto a finish lapped intermediate layer of Inconel. Eight rotors were also delivered with molybdenum disulfide deposited as a thin film lubricant on the spherical surface.

SECTION 3

TASK REVIEW

3.1 Task 1

Design and development of fixturing necessary to obtain non-destructible rotor and cavity parts.

3.1.1 Lapping Fixtures

Fixturing previously developed for the fabrication and finishing of opposed hemisphere type gas bearing parts was adapted to MESG-size parts. Masters for the calibration of CSDL gages were obtained and cross-calibrated with MESG processing equipment at Northrop PPD to insure that CSDL measurements would be comparable to those taken by others on similar hardware. The CSDL 3-Lap fixture for lapping spherical inner bearing parts was shown to be satisfactory for the preliminary lapping of MESG rotor parts. Anisotropic properties of the extruded beryllium material required that the final lapping of MESG rotor parts be done at elevated temperatures in order to insure sphericity at the unit operating temperature. A 2-Lap fixture was manufactured directly according to prints received from Autonetics. CSDL capability for the processing of MESG bearing parts was demonstrated.

3.1.2 Coating Fixtures

Previously used coating systems were readily adaptable to MESG in most cases by simply revising the holders for the rotor and cavity parts. This was particularly true for deposits by high-rate evaporation and conventional sputtering. Because of the complete spherical shape of the MESG rotor, it was considered necessary to use a hollow-cathode-type sputtering system in order to insure complete and uniform coverage by the deposit.

The hollow-cathode-type system commonly referred to as a sputter gun* employs a hollow cylindrical cathode and a passive anode as shown in Figure 3-1. As soon as the discharge is struck, electrons are trapped in a torroidal envelope just off the cathode surface by a non-linear magnetic field and are caused to spiral in front of the cathode face causing optimized ionization and high sputtering rates for conductive materials. The distribution of sputter material, also shown in Figure 3-1, was considered optimum for the coating of spherical bearing parts.

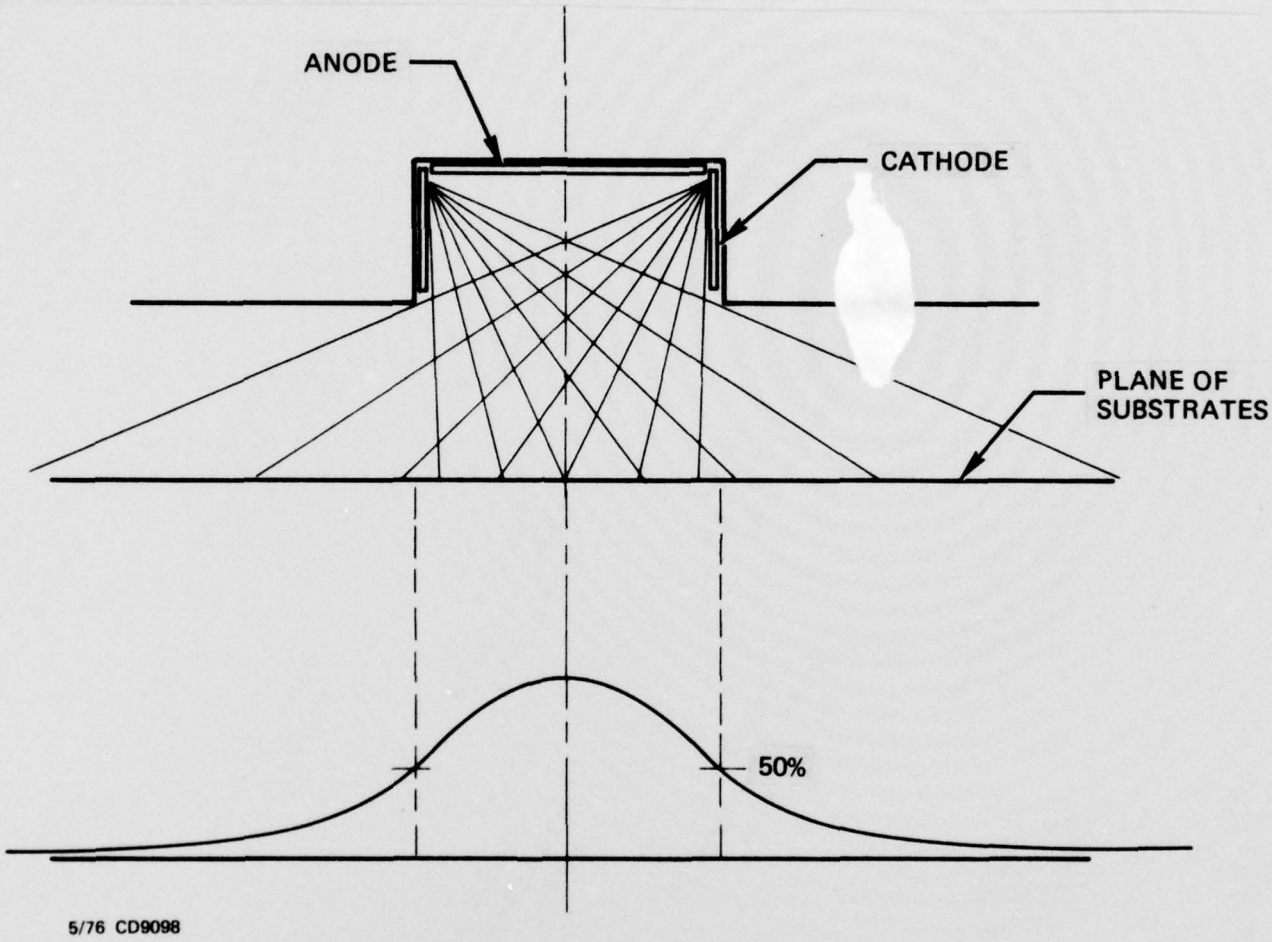

Figure 3-1. Model S-310 dc sputter gun - distribution of sputtered material.

*Manufactured by Sloan Technology Corporation of Santa Barbara, California 93103.

3.1.3 Wear Test Fixture

A turbo-molecular vacuum pump (Airco-Temescal, Model No. TMP-514) was used as the base for the wear tester. This pump features a rotor speed of 400 cycles/s and vacuum pressures below 1×10^{-7} torr are readily obtained. A cross-sectional view of the wear tester is shown in Figure 3-2. The rotating specimen is mounted securely on the top surface of the turbo pump rotor. Two capacitance transducers spaced 90 degrees apart from one another on the same radial plane are provided to detect any rotor unbalance resulting from the specimen mass and also to provide an accurate measure of rotor speed. Modified stainless steel pipe fittings (no. 304) were used to fabricate the vacuum chamber which includes ports for vacuum gauging and accessory feed-throughs. The stationary specimen and support assembly is mounted on the chamber top plate. A calibrated flexure mount holds the stationary specimen so that dimensional misalignments in the specimen wear surface can be compensated for and loading of the specimen surfaces can be accomplished. The flexure mount and specimen assembly is raised and lowered by a precision 1/4-80 threaded lead screw which is driven from outside of the vacuum chamber through a bellows-sealed rotary feed-through and slip coupling.

Testing was accomplished by mounting the specimens in their respective positions and establishing a vacuum below 5×10^{-6} torr. Rotor speed as indicated by capacitance probe readout was recorded. The stationary specimen was lowered until contact was made with the rotating specimen and then the lead screw was advanced a specified amount, causing a deflection in the flexure mount, thereby applying a load on the surfaces being tested. Initial surface contact and significant wear events were indicated by changes in the capacitance probe output which was displayed as a sine wave on an oscilloscope. This wave was caused by a change in distance between the probe face and the surface being sensed. Eccentricity of the surface being sensed with respect to the rotor spin axis produced a sinusoidal frequency equal to rotor speed. A comparison of this output with that of a standard frequency generator was an accurate determination of speed in revolutions per second. At the end of the period of contact, the stationary specimen was withdrawn and examined.

The choice of beryllium and beryllium oxide as specimen substrate materials was dictated by instrument requirements. Substrate blanks in the form of rings with an internal diameter of 2.05 inches and an external diameter of 2.55 inches were manufactured from S-200 structural grade

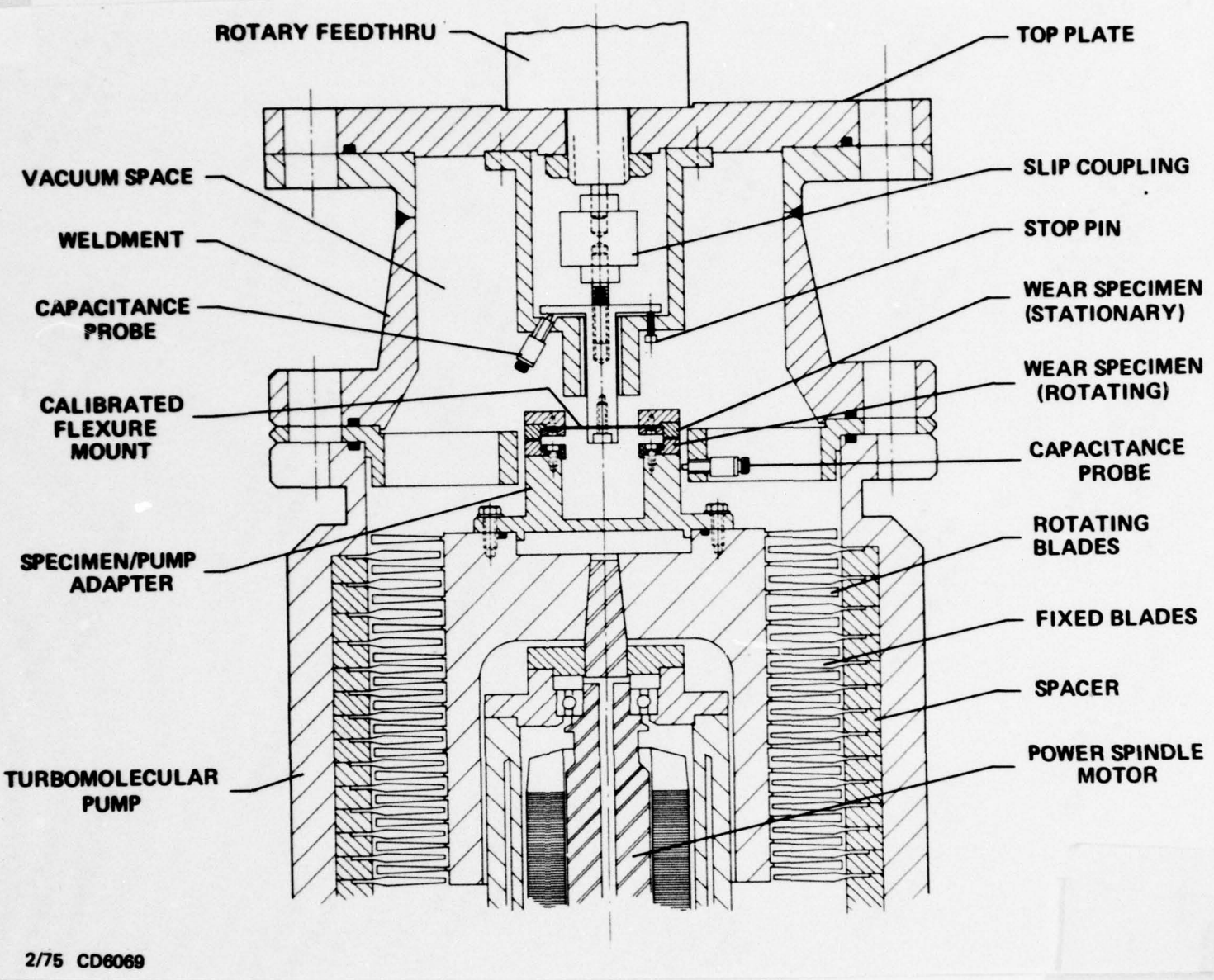

Figure 3-2. High speed wear tester.

beryllium and 99.5 percent dense beryllium oxide. Wear surfaces on the beryllium substrates were lapped using procedures similar to those developed to prepare optical surfaces. Wear surfaces on the beryllium oxide substrates were prepared using diamond lapping techniques. Centerline average roughness on beryllium substrates was less than 0.025 micrometer.

It was found that in order to insure proper specimen surface contact, loads of 50 – 100 grams were necessary, instead of the 10 gram load which more closely simulates MESG conditions. This was overcome by changing the test specimen configuration from a flat-on-flat type to a shoe-on-flat type, where load and momentary contact could be more closely controlled. Figure 3-3 schematically describes this test set-up.

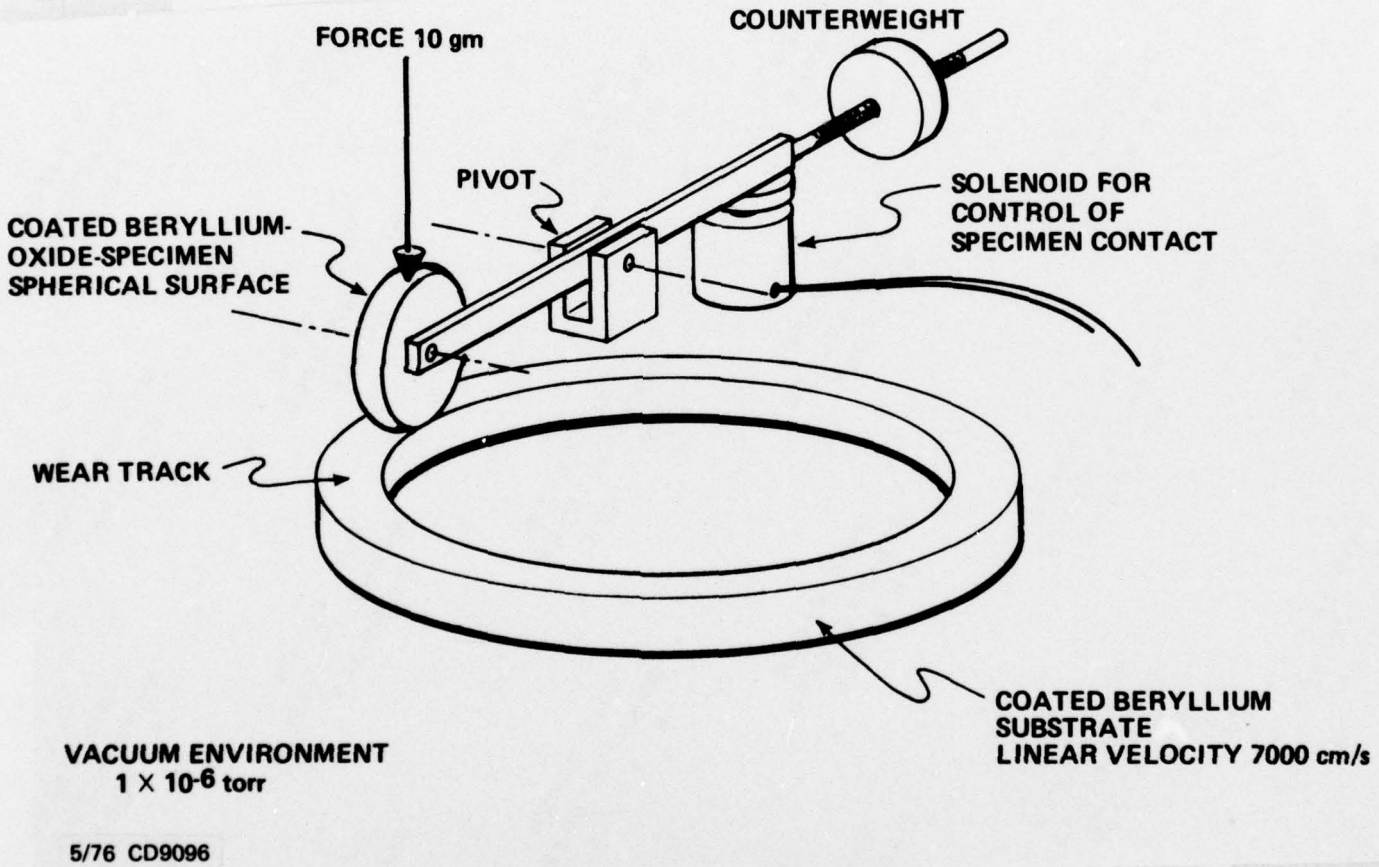

Figure 3-3. Schematic for shoe- and disc-type wear test.

The rotating specimen is in the form of a ring with a coating applied to a lapped face. The stationary specimen which simulates the MESG cavity is beryllium oxide in the form of a 1.0-inch diameter disc.

CUT HERE AND USE AS GUIDE FOR 10 X 15 INCH STRAIGHT EDGE AND 8 1/2 X 11 INCH PAPER

3/8 GRIPPER MARGIN 1/4 TOP EDGE OF IMPRESSION PAPER 1/4 GRIPPER MARGIN 3/8

ONE INCH

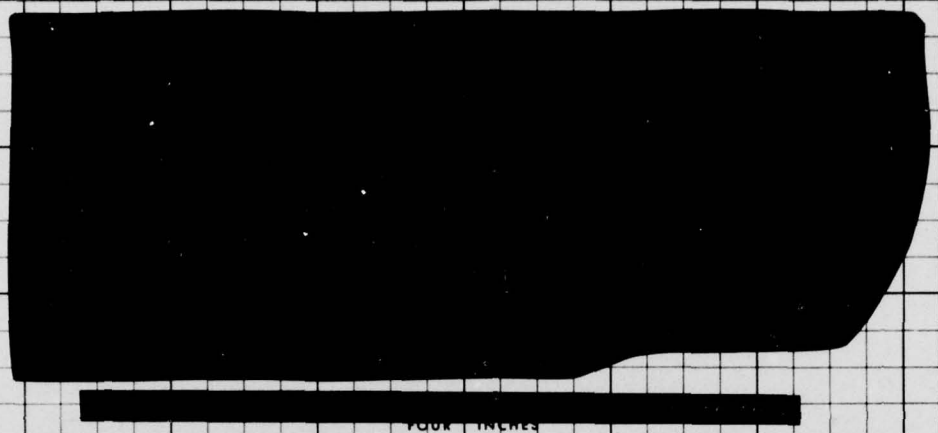

FOUR INCHES

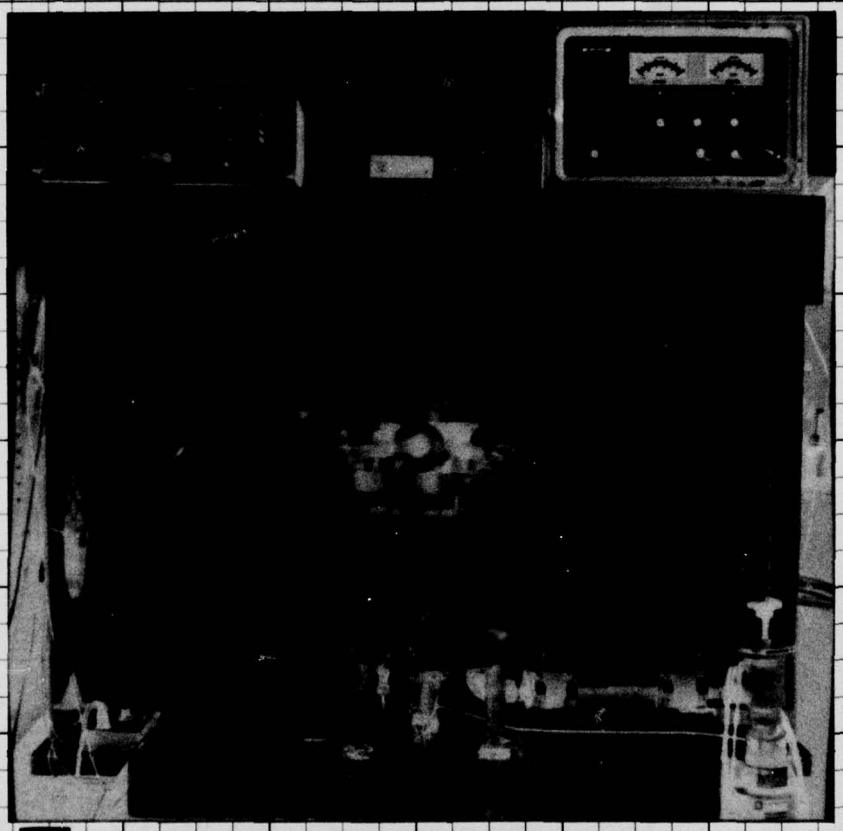

4 INCHES

3 INCHES

3 INCHES

4 INCHES

ONE INCH

BOTTOM OF ELEVEN INCH SHEET

TWELVE INCHES

THIRTEEN INCHES

GUIDE FOR RIGHT EDGE OF PLATE

GUIDE FOR RIGHT EDGE OF PLATE

IF MAXIMUM PRINTING AREA OF DUPLICATOR IS 13 INCHES LONG—KEEP IMAGE ABOVE THIS LINE

FIG. 3-4
Pg -12

3.2 Task 2

Coating, finishing, testing and evaluation of specimens to determine optimum coating and surface finish.

3.2.1 dc Sputtering

The phenomenon called sputtering refers to the planned erosion of the cathode electrode of a system by the bombardment of ionized gas molecules, usually argon. This is made to occur by passing an electrical discharge between electrodes at a low gas pressure. The eroded material leaves the cathode as free atoms to be condensed on surrounding surfaces. A diagram of the system used to apply coatings by sputtering is shown in Figure 3-5. Substrates were mounted on a rotatable holder and positioned to pass under the centerof a 2-inch diameter sputtering target. Rotation speed was approximately 5.0 cm diameter sputtering target. Rotation used to coat three-dimensional bearing parts. Prior to deposition, the specimen substrate surface was etched to achieve a high level of adhesive by applying a (-) dc voltage for a short time.

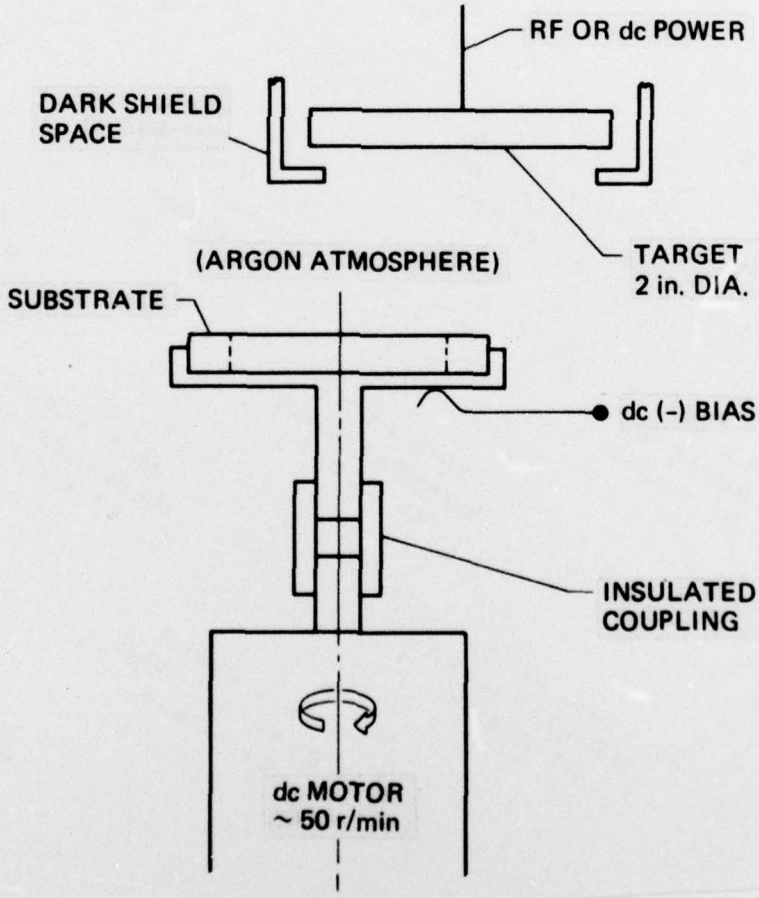

Figure 3-5. Diagram of system for the deposition of wear resistant coatings by sputtering.

3.2.2 Activated Reactive Evaporation Process (ARE)

Titanium carbide films can be deposited in thicknesses ranging from 10^{-6} up to 10^{-3} meters while mixtures of titanium and titanium carbide can be deposited in thicknesses greater than 0.5×10^{-3} meters. The objective is to deposit the minimum thickness necessary to satisfy surface finish and dimensional requirements. The activated reactive evaporation process was used to deposit these materials and is shown schematically in Figure 3-6. The process consists of a reaction between metal vapor atoms and gas molecules resulting in the formation and deposition of a compound. Metal vapor density is provided by two electron-beam heated pools of molten titanium in water-cooled copper crucibles. The reactive gas, acetylene, is introduced and directed toward the substrate surface. Activation of the reactants occurs when a yoke-shaped electrode above the pools is set to a positive potential. The substrate is heated by a dc resistance-type heater and is rotated slowly (1.8 r/min) to simulate deposition onto shaped bearing parts. Titanium compounds deposited in this manner show a large grained 100 percent titanium carbide structure when examined by x-ray diffraction techniques.

3.2.3 Wear Test Results

Material combinations and coating properties used in the flat-on-flat type wear tests are summarized in Table 3-1.

Coated beryllium specimens rotating at 400 revolutions per second were brought into contact with coated beryllium oxide surfaces with an approximate force of 10 grams and in a vacuum of 7×10^{-7} torr. In all cases, significant wear tracks resulted in both members of the combination. The deepest tracks occurred in the coated beryllium surfaces while tracks of lesser depth were found in the thicker titanium carbide films on beryllium oxide. Elemental identification of the material present in the wear tracks by x-ray energy determination with an energy dispersive x-ray spectrometer on the scanning electron microscope showed that measureable amounts of material were transferred from one surface to the other. It also showed that significant amounts of the sputter deposited material were removed from the wear track area.

The initial contact in the testing of combinations 1 and 5 resulted in an excessively high level of friction. In both tests the stationary specimen flexure mount was damaged, which in turn resulted in a higher than desired contact load that caused the removal of most of the

Table 3-1. Test material combinations and coating properties.

Comb No.	Specimen No.	*	Material	Process	Thickness (μ-m)	Hardness Knoop 100 gm load	Surface finish CLA (μ-m)
1	4-7	S	TiC	A.R.E.	125.0	1200	.055-.067
	3-50	R	WC+Co	dc sput	.50	-	.005-.015
2	4-33	S	TiC	A.R.E.	100.0	1650	.08-.09
	3-47	R	WC+Co	dc sput	1.88	-	.010-.020
3	4-10	S	WC+Co	dc sput	3.76	-	.10-.15
	3-48	R	WC+Co	dc sput	1.00	-	.02-.025
4	4-33	S	TiC	A.R.E.	50.0	1450	.04-.05
	4-41	R	WC	dc sput	3.0	-	.15-.17
5	4-44	S	TiC	A.R.E.	150.0	1000	.15
	3-68	R	TiC	dc sput	.50	-	.012-.022

* S - Stationary
  R - Rotating

** A.R.E. - Activated Reactive Evaporation

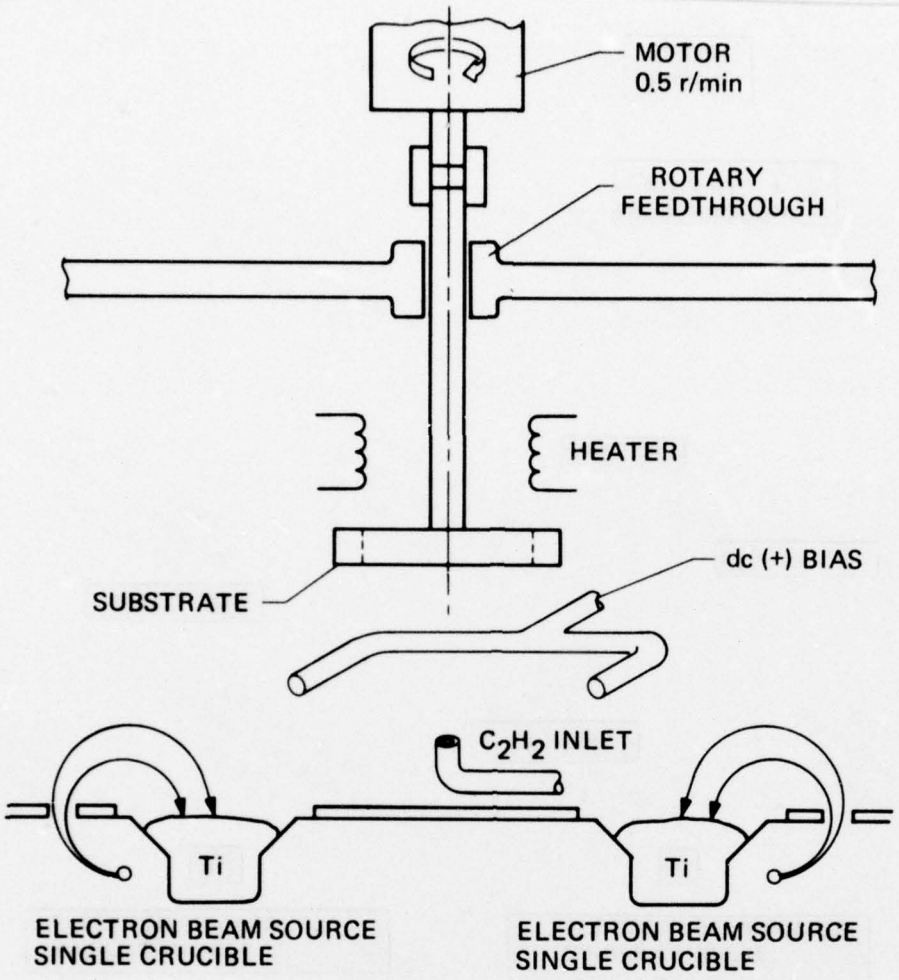

Figure 3-6. Schematic of system for the deposition of titanium carbide by activated reactive evaporation.

sputtered coatings from the wear track area. Wear tracks and elemental analysis data from test combination 1 are shown in Figure 3-7. The wear track in the titanium carbide surface appears as a layer of smeared material while the wear track in the tungsten carbide-cobalt surface is quite smooth by comparison. Cracks formed in the beryllium substrate of the tungsten carbide-cobalt sample, perpendicular to the direction of the wear track. Energy dispersive x-ray analysis showed that most of the sputtered coating was removed from the wear track area in the tungsten carbide-cobalt surface and that a significant amount of titanium had transferred to the surface.

3/8 GRIPPER MARGIN 1/4 TOP EDGE OF IMPRESSION PAPER 1/4 GRIPPER MARGIN 3/8

ONE INCH

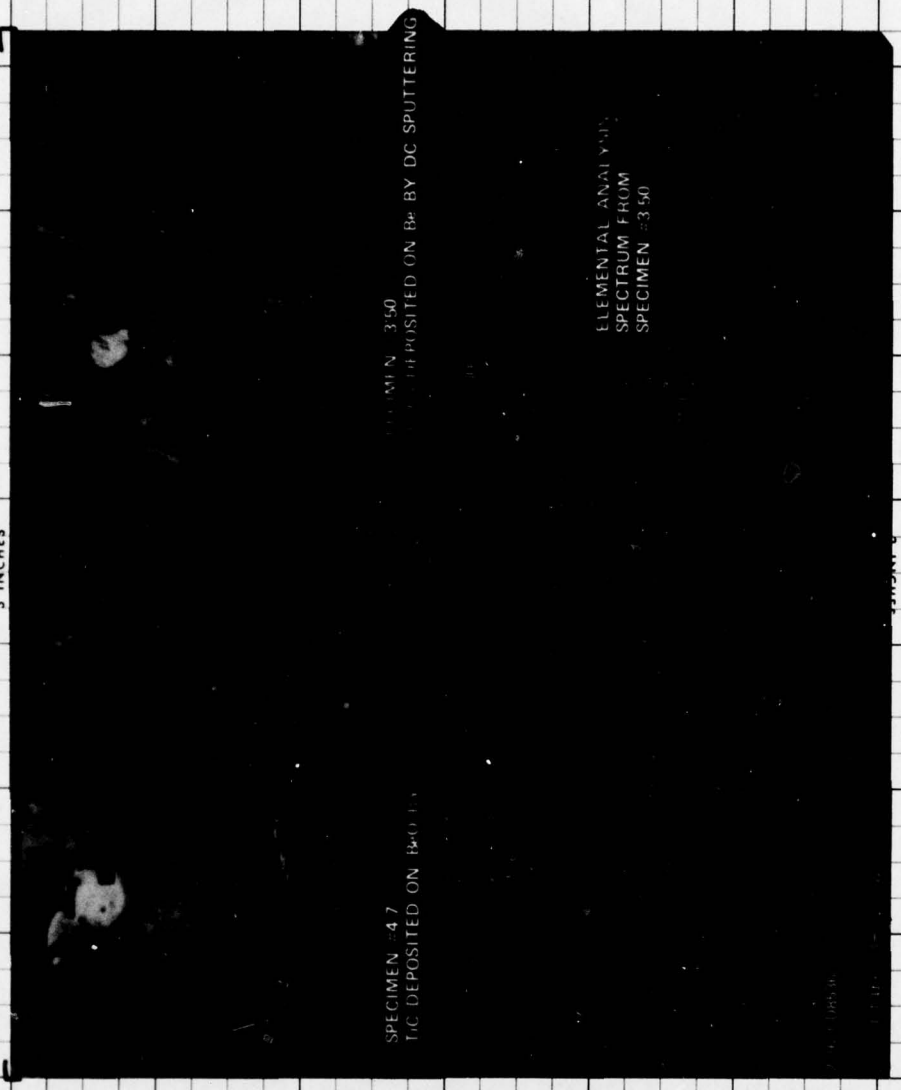

4 INCHES

3 INCHES

4 INCHES

GUIDE FOR RIGHT EDGE OF PLATE

TEN INCHES

BOTTOM OF ELEVEN INCH SHEET

TWELVE INCHES

THIRTEEN INCHES

FIG. 3-7
Pg-17

IF MAXIMUM PRINTING AREA OF DUPLICATOR IS 13 INCHES LONG—KEEP IMAGE ABOVE THIS LINE

GUIDE FOR RIGHT EDGE OF PLATE

masking

DATE ORDER NO.

TAYLOR

Results were similar for test combination 2. Specimen loading was approximately 10 grams for a period of 60 seconds. Wear track characteristics are similar to those of test combination 1, but to a lesser degree. The resulting wear tracks and energy dispersive x-ray analysis spectrum in Figure 3-8 show that titanium was transferred to the titanium carbide-cobalt coating and that tungsten is present on the surface of the titanium carbide coating. The titanium carbide surface was repolished to remove all traces of wear and reused in test combination 4.

Test combination 3 differs in that sputter deposited tungsten carbide-cobalt is used as the coating on both the beryllium and beryllium oxide surfaces. The tungsten carbide-cobalt surface as deposited on beryllium oxide is shown in Figure 3-9 with typical voids which are due to inherent porosity and pull-out characteristics of the lapped beryllium oxide surface. Wear tracks resulting from contact with specified load and vacuum for a period of approximately 60 seconds are shown in Figure 3-10. Disrupted particles are shown on the coated beryllium surface and pull-out also appears on the coated surface of the beryllium oxide stationary member. Using dispersive x-ray analysis a comparison of the major peak intensities of the coatings on the wear track and on the as-coated surface shows that over 90 percent of the coating has been removed from the wear track.

Test combination 4 considers the effect of cobalt in the tungsten carbide coatings. Surface contact was maintained for 10 seconds at the specified speed, load and vacuum with results similar to those obtained with test combination 2. Figure 3-11 shows a deep wear track on the tungsten carbide coated beryllium member with little of the tungsten carbide coating remaining. Energy dispersive x-ray data shows titanium from the titanium carbide coated beryllium oxide member in the wear track area.

Test combination 5 was included to observe the effect of using sputter deposited titanium carbide in place of the tungsten carbide-cobalt mixture used in the preceding tests. Surface contact at the specified speed, load and vacuum resulted in high friction forces which damaged the flexure mount and resulted in deep wear tracks similar to those observed at the end of test no. 1.

Previously prepared beryllium oxide and beryllium substrates were coated and wear tested using the shoe-on-disc type of test. Molybdenum

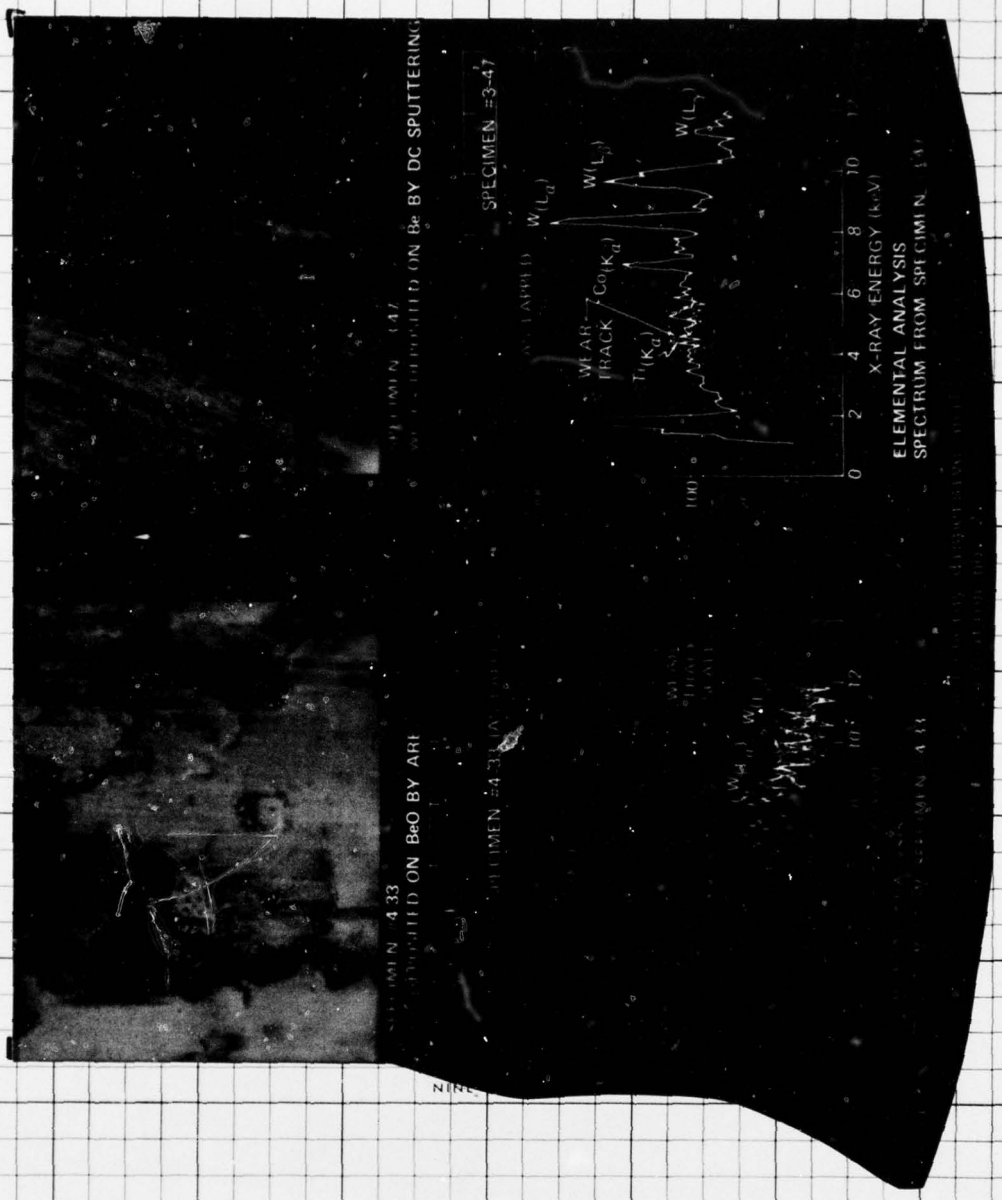

FIG. 3-8
Pg 19

3/8 GRIPPER MARGIN 1/4 TOP EDGE OF IMPRESSION PAPER 1/4 GRIPPER MARGIN 3/8

ONE INCH

4 INCHES

3 INCHES

2 INC

3 INCHES

4 INCHES

TEN INCHES

BOTTOM OF ELEVEN INCH SHEET

TWELVE INCHES

THIRTEEN INCHES

FIG. 3-9

Pg-20

GUIDE FOR RIGHT EDGE OF PLATE

GUIDE FOR RIGHT EDGE OF PLATE

IF MAXIMUM PRINTING AREA OF DUPLICATOR IS 13 INCHES LONG—KEEP IMAGE ABOVE THIS LINE

masking

DATE ORDER NO.

TAYLOR

3/8 GRIPPER MARGIN 1/4 TOP EDGE OF IMPRESSION PAPER 1/4 GRIPPER MARGIN 3/8

ONE INCH

INCHES

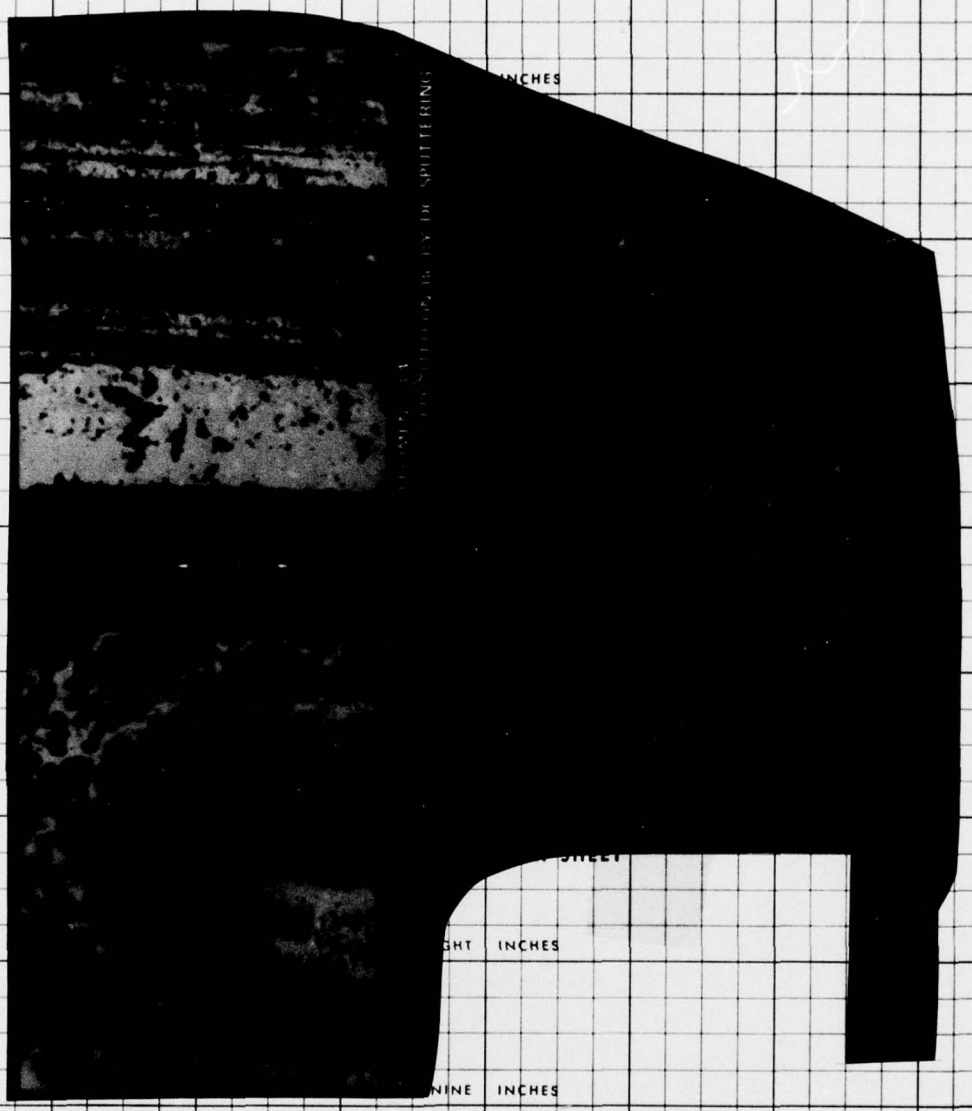

4 INCHES

4 INCHES

GHT INCHES

NINE INCHES

TEN INCHES

BOTTOM OF ELEVEN INCH SHEET

TWELVE INCHES

THIRTEEN INCHES

IF MAXIMUM PRINTING AREA OF DUPLICATOR IS 13 INCHES LONG—KEEP IMAGE ABOVE THIS LINE

GUIDE FOR RIGHT EDGE OF PLATE

GUIDE FOR RIGHT EDGE OF PLATE

Fig. 3-10

PS-21

3/8 GRIPPER MARGIN 1/4 TOP EDGE OF IMPRESSION PAPER 1/4 GRIPPER MARGIN 3/8

ONE INCH

TWO INCHES

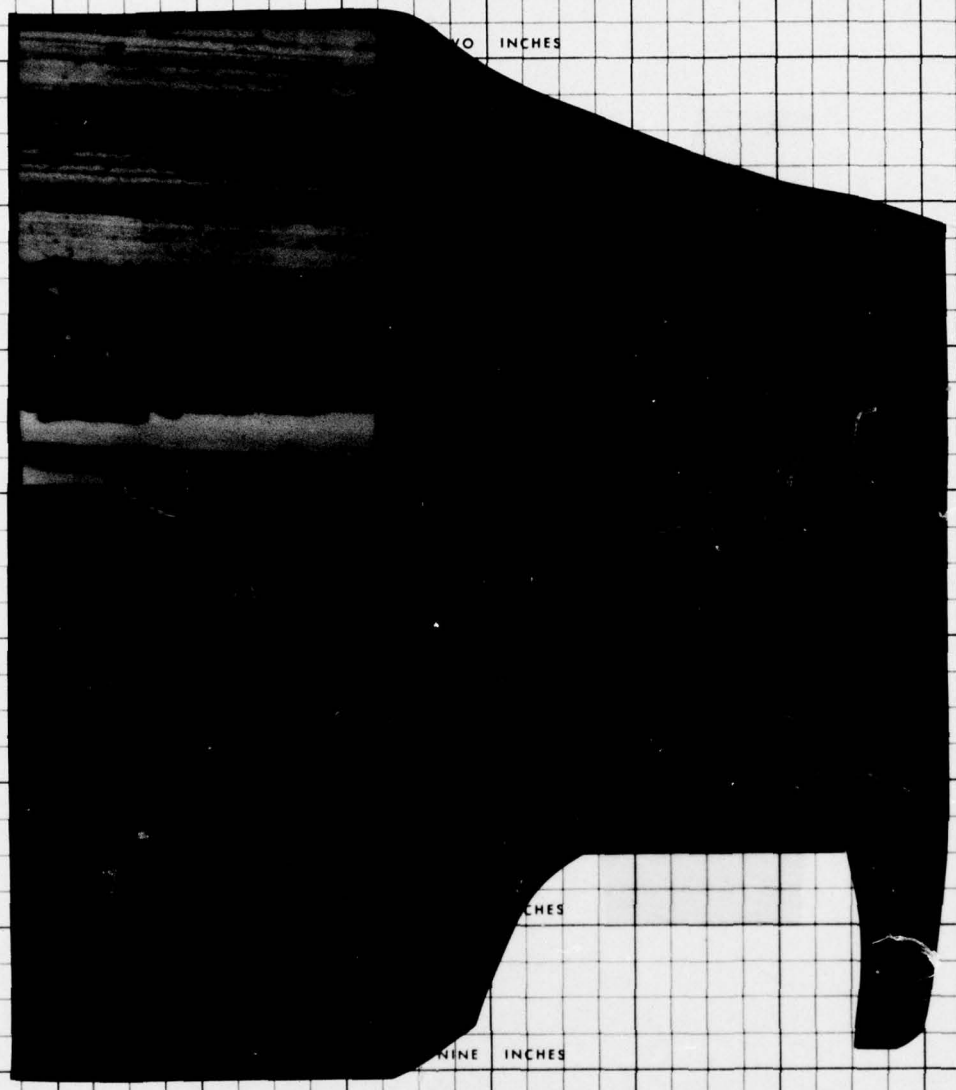

4 INCHES

4 INCHES

NINE INCHES

TEN INCHES

BOTTOM OF ELEVEN INCH SHEET

TWELVE INCHES

THIRTEEN INCHES

GUIDE FOR RIGHT EDGE OF PLATE

GUIDE FOR RIGHT EDGE OF PLATE

IF MAXIMUM PRINTING AREA OF DUPLICATOR IS 13 INCHES LONG—KEEP IMAGE ABOVE THIS LINE

DATE ORDER NO.

FIG. 3-11

Pg 22

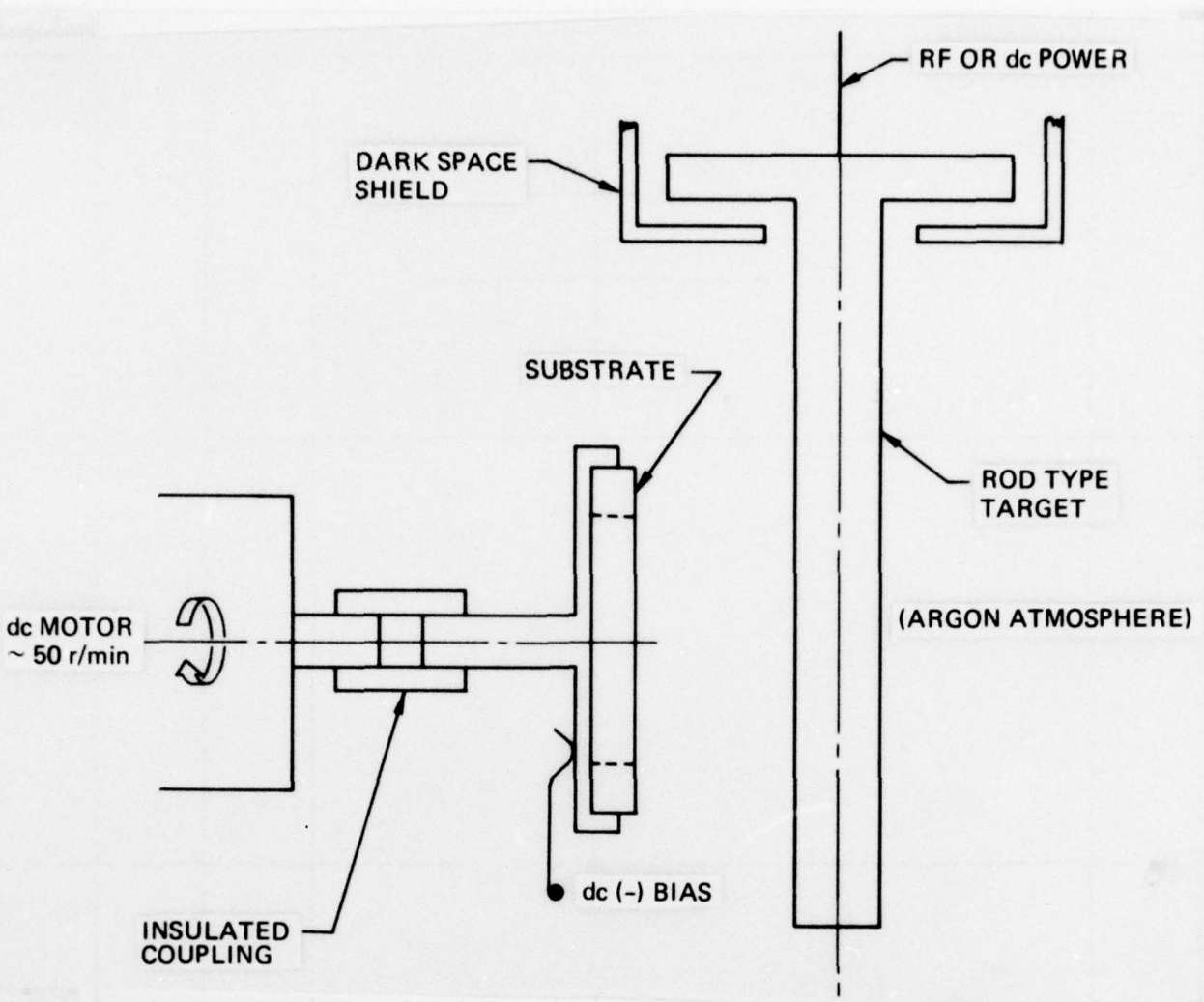

Figure 3-12. Diagram for the deposition of MoS_2 coatings on beryllium discs for shoe-on-disc type wear test.

Precise positioning of the specimens in the wear tests allowed each of the carbide coatings to be tested with each of the three MoS_2 coatings. Table 3-2 contains the coating properties and Figure 3-14 shows surface topography and coating thickness data as obtained with a Bendix Proficorder System for surface profilometry measurements. This data was obtained by traversing a mechanical stylus across the coated areas of the substrate surface.

Wear test data is shown in Figures 3-15, 3-16, and 3-17 for each of the nine combinations of the test specimen. The photomicrographs of the wear locations show that MoS_2 was transferred from the rotating to stationary surface in each case and the magnitude of material transfer is dependent on the thickness of the MoS_2 deposit. Rotating disc no. S-36 had the thinnest MoS_2 film based on deposition time and the resulting wear tracks and spots were much smaller than those shown for the

other two cases. The coated beryllium oxide surface showed little or no wear after the removal of transferred materials. These materials deposited by sputtering appear to be promising choices for the MESG application.

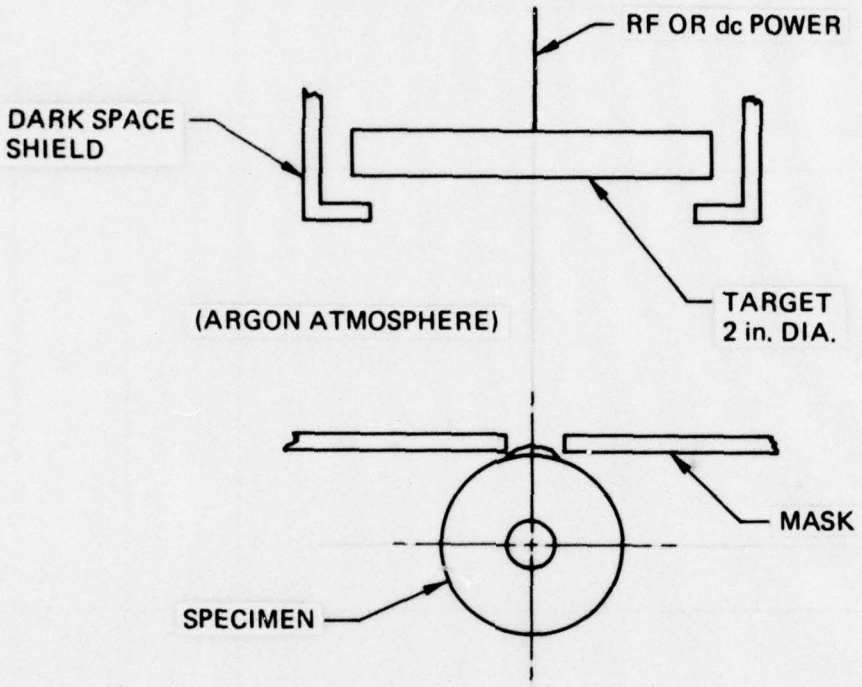

Figure 3-13. Diagram for the depositon of wear resistant coatings.

3.2.4 Electrical Resistivity, Magnetic Susceptibility and Adhesion Test Results

Coating materials considered for use as cavity surfaces in the MESG instrument were required to be electrically conductive and nonmagnetic since the slightest magnetic field could cause unmodelable drift rates. Adhesion integrity is also essential to the success of any coating application and must be adequate to a-low for the precision sizing of the coated surface.

The substrate material used throughout this program is beryllium oxide. Its high thermal conductivity, electrical resistivity, and excellent dielectric properties make it suitable for structural applications requiring surface circuitry. The substrate size is 5.08 cm long by 2.54 cm wide by 0.0635 cm thick and the deposits cover one entire side.

Table 3-2. Test material and coating properties for shoe-on-disc type wear tests.

Stationary: Beryllium Oxide Specimens

Specimen No.	Material	Sputtering Time (minutes)	Thickness µin.	Density Rate /mm	Plasma
1	WC+Co	180	1.5	0.0083	Argon
2	WC+Co+TiC (outer layer)	180 60	1.5 0.25	0.0083 0.0042	Argon
3	TiC+Ni	180	0.63	0.0035	Argon

Rotating: Beryllium Specimens

Specimen No.	Material	Sputtering Time (minutes)	Thickness µin.	Density Rate /mm	Plasma
3-47	MoS_2	60	—	—	Argon
5-36	MoS_2	50	—	—	H_2S
5-37	MoS_2	37	—	—	H_2S

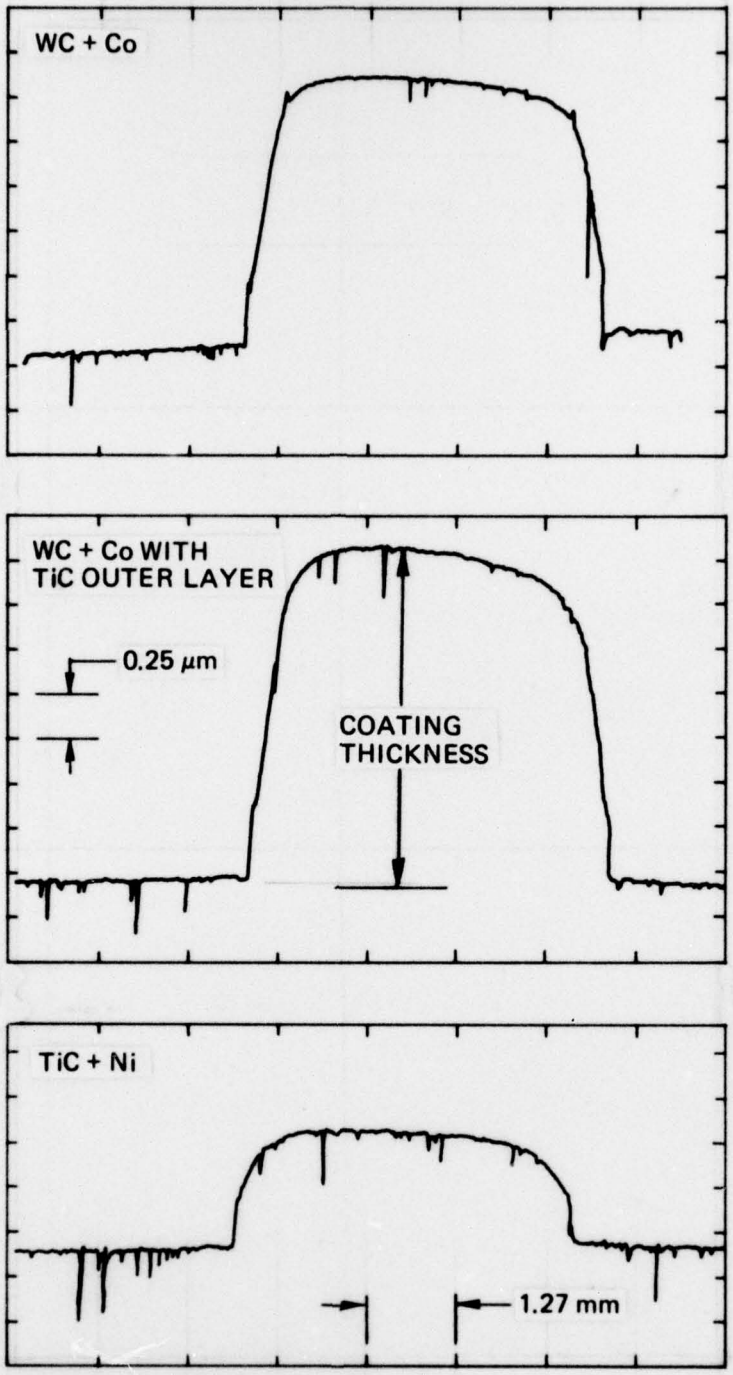

Figure 3-14. Surface profiles for coated areas on beryllium oxide substrate as coating specimens for wear tests.

3/8 GRIPPER MARGIN 1/4 TOP EDGE OF IMPRESSION PAPER 1/4 GRIPPER MARGIN 3/8

ONE INCH

4 INCHES

4 INCHES

GUIDE FOR RIGHT EDGE OF PLATE

TEN INCHES

BOTTOM OF ELEVEN INCH SHEET

TWELVE INCHES

THIRTEEN INCHES

FIG 3-15
PG 27

IF MAXIMUM PRINTING AREA OF DUPLICATOR IS 13 INCHES LONG—KEEP IMAGE ABOVE THIS LINE

GUIDE FOR RIGHT EDGE OF PLATE

masking

A.B.DICK

DATE ORDER NO.

CUSTOMER TAYLOR

3/8 GRIPPER MARGIN 1/4 TOP EDGE OF IMPRESSION PAPER 1/4 GRIPPER MARGIN 3/8

ONE INCH

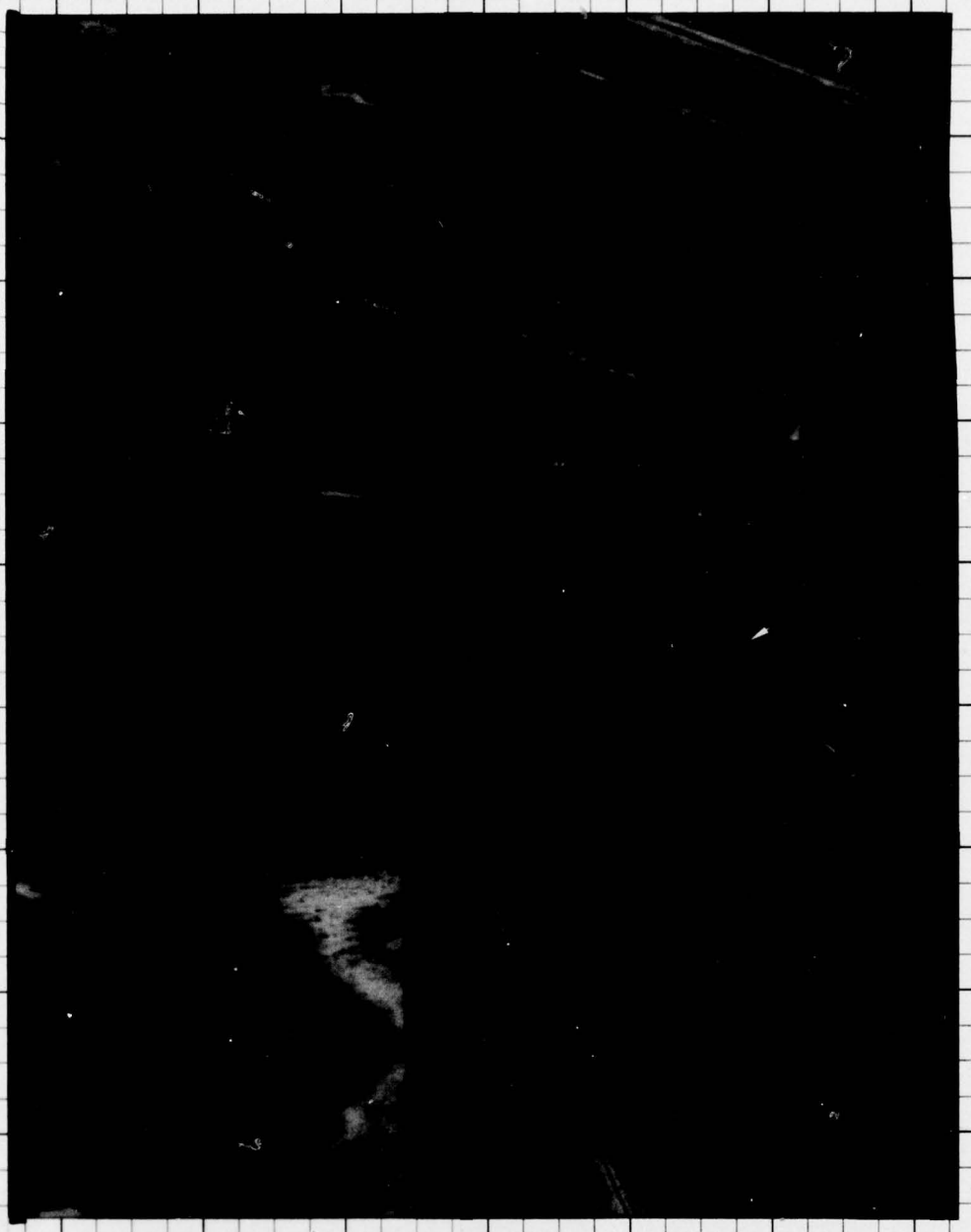

4 INCHES

4 INCHES

GUIDE FOR RIGHT EDGE OF PLATE

TEN INCHES

BOTTOM OF ELEVEN INCH SHEET

TWELVE INCHES

FIG 3-16

Pg 28

THIRTEEN INCHES

IF MAXIMUM PRINTING AREA OF DUPLICATOR IS 13 INCHES LONG—KEEP IMAGE ABOVE THIS LINE

GUIDE FOR RIGHT EDGE OF PLATE

masking

DATE ORDER NO.

TAYLOR

3/8 GRIPPER MARGIN 1/4 TOP EDGE OF IMPRESSION PAPER 1/4 GRIPPER MARGIN 3/8

ONE INCH

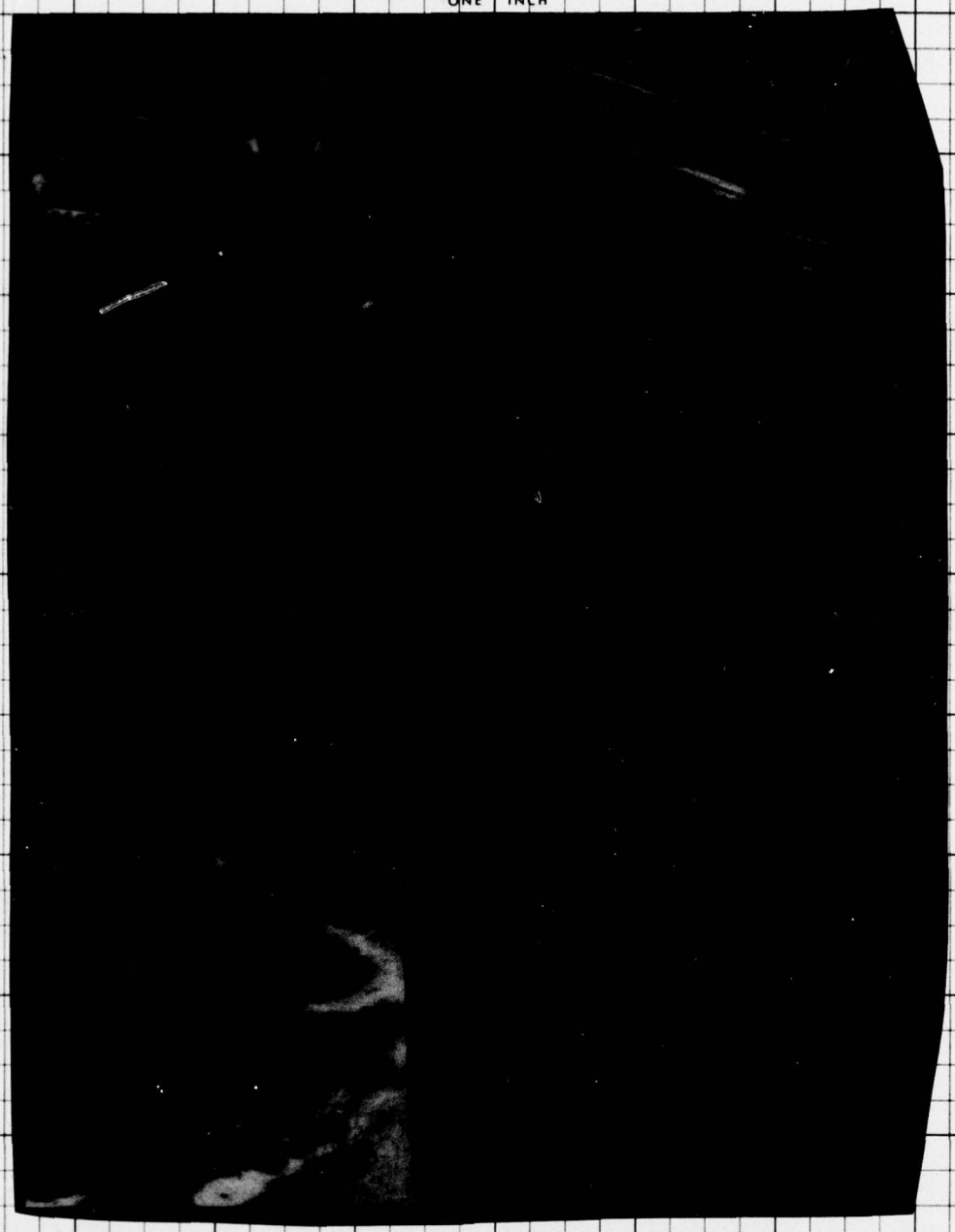

4 INCHES

4 INCHES

GUIDE FOR RIGHT EDGE OF PLATE

TEN INCHES

BOTTOM OF ELEVEN INCH SHEET

TWELVE INCHES

THIRTEEN INCHES

FIG. 3-17
Pg 29

IF MAXIMUM PRINTING AREA OF DUPLICATOR IS 13 INCHES LONG—KEEP IMAGE ABOVE THIS LINE

GUIDE FOR RIGHT EDGE OF PLATE

masking

DATE ORDER NO.

CUSTOMER

Tungsten carbide and tungsten carbide with cobalt deposits were applied by dc sputtering. The substrates were mounted in a rotating holder in such a manner as to allow complete coverage of the exposed side using a 5.0-cn-diameter target. Titanium carbide was also sputter-deposited using RF sputtering techniques in a commercial planar-diode system, also adapted to use 5.0-cm-diamter targets and titanium carbide was also deposited by activated reactive evaporation. Titanium was evaporated from two sources simultaneously and activated by suitable biasing in a reactive acetylene atmosphere to deposit as titanium carbide on the slowly rotating substrate. Table 3-3 summarizes the physical properties of the deposits.

Table 3-3. Physical properties of specimen deposits.

SPECIMEN NO.	MATERIAL	PROCESS	THICKNESS (μm)	CROSS-SECTION ($cm^2 \times 10^3$)	DEPOSITION RATE (Å/min)
1	WC + Co	dc sput.	3.00	0.724	167
2	WC	dc sput.	2.50	0.603	140
3	TiC	RF sput.	0.75	0.101	42
4	TiC	ARE*	60.00	14.50	25000

*Activated Reactive Evaporation

Figure 3-18 through 3-21 are photomicrographs obtained by scanning electron microscopy showing the surface texture and cross-sectional structure of the coating. Figures 3-18 and 3-19 show similar texture and structure for both tungsten carbide with similar texture and structure for both tungsten carbide of the beryllium-oxide substrate provides provides preferential nucleation sites resulting in the formation of a complex nodular structure. This type of structure is also demonstrated for the thinner titanium-carbide film shown in Figure 3-20. A thick film of titanium carbide deposited by activated reactive evaporation is shown in Figure 3-21. A dense columnar structure is shown in the fracture cross section.

3/8 GRIPPER MARGIN 1/4 TOP EDGE OF IMPRESSION PAPER 1/4 GRIPPER MARGIN 3/8

ONE INCH

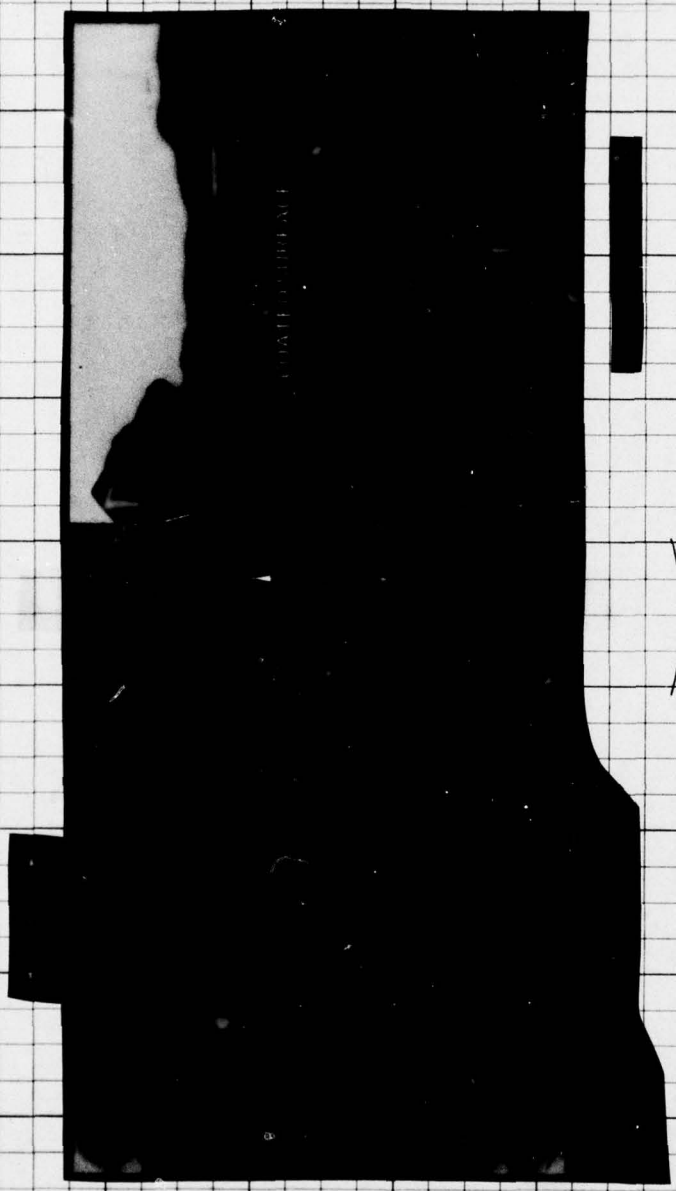

4 INCHES

2 INCHES

2 INCHES

3 INCHES

4 INCHES

TEN INCHES

BOTTOM OF ELEVEN INCH SHEET

TWELVE INCHES

THIRTEEN INCHES

GUIDE FOR RIGHT EDGE OF PLATE

GUIDE FOR RIGHT EDGE OF PLATE

IF MAXIMUM PRINTING AREA OF DUPLICATOR IS 13 INCHES LONG—KEEP IMAGE ABOVE THIS LINE

DATE ORDER NO.

FIG. 3-18

Pg-31

3/8 GRIPPER MARGIN 1/4 TOP EDGE OF IMPRESSION PAPER 1/4 GRIPPER MARGIN 3/8

ONE INCH

4 INCHES

3 INCHES

2 INCHES

3 INCHES

4 INCHES

GUIDE FOR RIGHT EDGE OF PLATE

TEN INCHES

BOTTOM OF ELEVEN INCH SHEET

TWELVE INCHES

THIRTEEN INCHES

FIG. 3-19

Pg 32

IF MAXIMUM PRINTING AREA OF DUPLICATOR IS 13 INCHES LONG—KEEP IMAGE ABOVE THIS LINE

GUIDE FOR RIGHT EDGE OF PLATE

masking

DATE ORDER NO.

TAYLOR

CUSTOMER

3/8 GRIPPER MARGIN 1/4 TOP EDGE OF IMPRESSION PAPER 1/4 GRIPPER MARGIN 3/8

ONE INCH

FIVE INCHES

4 INCHES | 3 INCHES | 2 INCHES | 1 INCH | ER OF | 1 INCH | 2 INCHES | 3 INCHES | 4 INCHES

ELEVEN INCH SHEET

SIX INCHES

TEN INCHES

BOTTOM OF ELEVEN INCH SHEET

TWELVE INCHES

THIRTEEN INCHES

IF MAXIMUM PRINTING AREA OF DUPLICATOR IS 13 INCHES LONG—KEEP IMAGE ABOVE THIS LINE

GUIDE FOR RIGHT EDGE OF PLATE

GUIDE FOR RIGHT EDGE OF PLATE

FIG. 3-20

~~Pg 34~~ Pg 33

masking

DATE ORDER NO.

TAYLOR

CUSTOMER

3/8 GRIPPER MARGIN 1/4 TOP EDGE OF IMPRESSION PAPER 1/4 GRIPPER MARGIN 3/8

ONE INCH

INCHES

R OF

4 INCHES 3 INCHES 2 INCHES 1 INCH 1 INCH 2 INCHES 3 INCHES 4 INCHES

ELEVEN INCH SHEET

TEN INCHES

BOTTOM OF ELEVEN INCH SHEET

TWELVE INCHES

THIRTEEN INCHES

GUIDE FOR RIGHT EDGE OF PLATE

GUIDE FOR RIGHT EDGE OF PLATE

IF MAXIMUM PRINTING AREA OF DUPLICATOR IS 13 INCHES LONG—KEEP IMAGE ABOVE THIS LINE

FIG. 3-21
Pg 34

masking

DATE ORDER NO.

CUSTOMER TAYLOR

3.2.4.1 Electrical Resistivity

Electrical resistivity is defined as the ratio of potential gradient in a conductor to the current density that is produced. It is numerically equal to the resistance offered by a unit cube of a substance. It can be expressed mathematically as

$$\rho = \frac{RA}{\ell} \qquad (1)$$

(see Reference 4)

where:

ρ = resistivity
R = resistance
A = cross-sectional area
ℓ = length

and the commonly used units are ohm-centimeters.

The resistivity of the four specimen deposits was measured using a conventional square four-point probe array as shown schematically in Figure 3-22. Voltage is applied to two adjacent points in the array causing current to flow through the deposit. The voltage drop resulting from resistance between the other two points in the array was measured and recorded. The resistivity of the deposit was calculated using the following relationship from Reference 5.

$$\rho = \frac{V}{I} \frac{2\pi}{\ell n\ 2} d \qquad (2)$$

where:

I = current flowing through the deposit
V = voltage drop recorded across the test points
d = deposit thickness expressed in centimeters

Experimental results obtained from three positions on each of the specimen deposits are given in Table 3-4.

The tabulated resistivity values show the effects of variation on the deposit thickness. The method of sputter deposition used to produce specimens 1 and 2 resulted in a slightly thicker deposit in the center of the specimen area which corresponded to position 2. Positions 1 and 3 are located toward the ends of the specimen area. Measurements

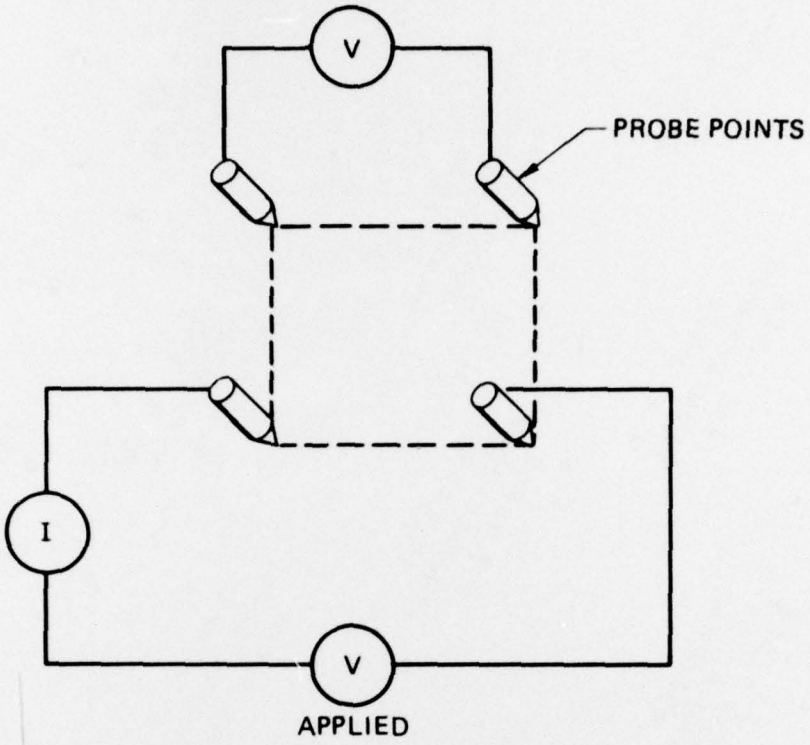

Figure 3-22. Square probe array for electrical-resistivity measurements.

Table 3-4. Electrical resistivity of specimen deposits.

SPECIMEN NO.	MATERIAL	THICKNESS (μm)	RESISTIVITY (Ω-cm)		
			POSITION 1	POSITION 2	POSITION 3
1	WC + Co	3.00	0.00124	0.00090	0.00124
2	WC	2.50	0.00061	0.00038	0.00062
3	TiC	0.75	0.00417	0.0130	0.0190
4	TiC	60.00	0.00048	0.00051	0.00048

The tabulated resistivity values show the effects of variation in the deposit thickness. The method of sputter

from specimen 3 show a significantly higher level of resistivity indicating that this deposit is quite thin and not fully formed. The low resistivity values obtained from deposit 4 show the effect of increased density and thickness of the deposit.

3.2.4.2 Magnetic Susceptibility

Magnetic susceptibility is used to characterize materials whose permeability differs from unity by a very small amount. It is defined as the ratio of the intensity of magnetization of the material to the strength of the magnetic-field intensity in the material. This is one of the more important magnetic parameters because it provides basic information about the ease with which the material can be magnetized.

The measurement of magnetic susceptibility requires the use of sensitive force-measuring equipment as minute mechanical forces are experienced by the specimen in a nonuniform magnetic field. This method is commonly referred to as the Gouy Method. A schematic of the test apparatus is shown in Figure 3-23. The specimen is hung from a sensitive balance with its major axis vertical and the lower end located in the uniform part of the magnetic field but above the centerline of of the pole pieces of the electromagnet. A force due to the presence of the magnetic field is measured by the balance. Magnetic susceptibility of the specimens was calculated using Equation (3) (see Reference 3).

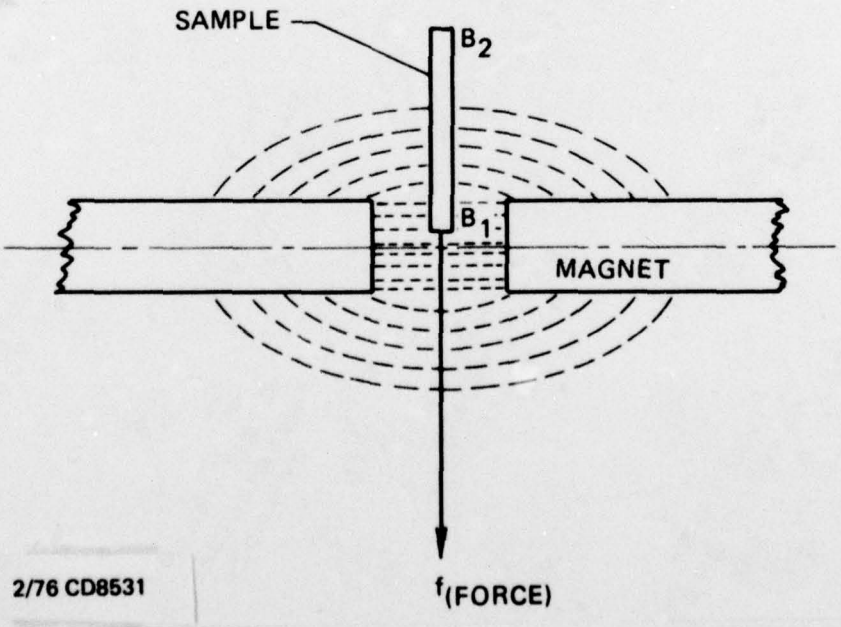

Figure 3-23. Schematic of the Gouy Method apparatus for measuring magnetic susceptibility.

$$K = \frac{2f}{A(B_1^2 - B_2^2)} \quad (3)$$

where:

K = susceptibility
f = force (dynes)
A = areas of specimens (cm^2)
B_1 = field at lower end (gauss)
B_2 = field at upper end (gauss)

The experimental results are summarized in Table 3-5. Tests conducted on specimens 1 and 4 did not produce a measurable force indicating that these deposits are extremely nonmagnetic. Tests conducted on specimen 2 showed a negative force as the specimen tended to be repelled by the magnetic field. This deposit can be considered a diamagnetic material.

Table 3-5. Magnetic susceptibility of specimen deposits.

SPECIMEN NO.	MATERIAL	THICKNESS (μm)	FORCE (dyn)	SUSCEPTIBILITY
1	WC + Co	3.00	0	0
2	WC	2.50	-2.06	-6.8×10^{-6}
3	TiC	0.75	1.47	16.2×10^{-6}
4	TiC	60.00	0	0

These materials have no permanent magnetic moment, but moments are induced by the influences of the magnetic field and have a direction opposite to that of the inducing field. This property is extremely small and is probably present in all materials. Specimen 3 produced a positive force of attraction when the magnetic field was applied. Materials with a positive susceptibility have a permanent magnetic moment, but the interatomic spacing is large and there is negligible atomic interaction. Although this effect is greater than the dismagnetic effect, it is still very small. Determination of the elemental composition of the deposits by energy-dispersive X-ray analysis on the

on the scanning electron microscope showed no unusual elements present in any of the deposits that would account for the observed differences in susceptibility data.

3.2.4.3 Adhesion Integrity

Fabrication ability and hardware reliability are related to adhesion integrity establishing a need for a test procedure that would assign some degree of measure to the bond of deposits to their substrates. A tensile-test procedure was established where the flat end-face of a 0.3-cm diameter pin is attached to the surface of the deposit using an epoxy cement as shown in Figure 3-24. A force is applied along the axis of the pin to pull it away from the deposit. An examination of the face of the pin showed degrees of adhesion ranging from a case where a large section of the beryllium-oxide substrate was sheared off, to cases where the strength of the epoxy cement bond was insufficient to remove the deposit from the substrate surface. The results of these tests are summarized in Table 3-6. In general, the majority of the tests' results showed both particles of the deposit on the face of the pin and on the substrate. A major limitation of this type of test is the difficulty in obtaining a cement joint with greater bond strength than that of the deposit and substrate.

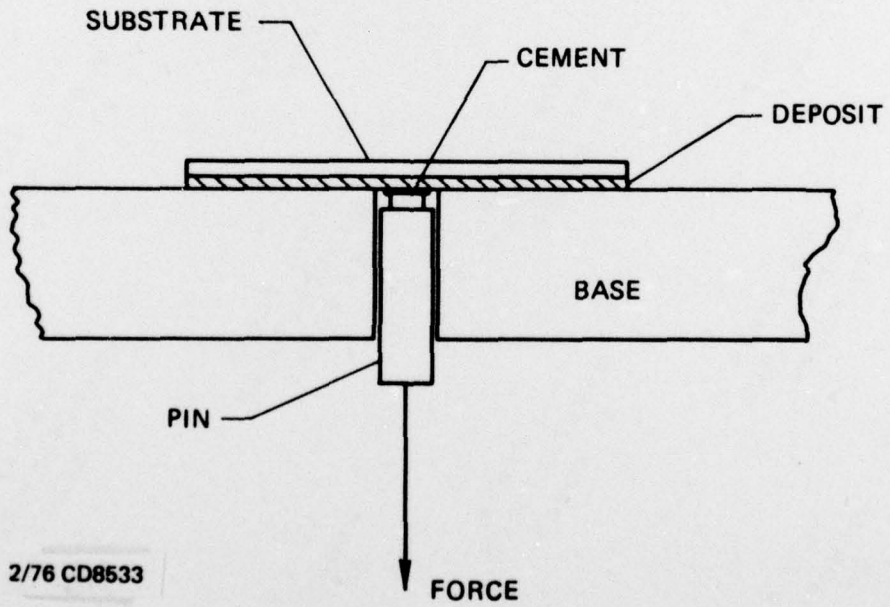

Figure 3-24. Schematic of pull-test setup for adhesion-integrity measurements.

Table 3-6. Adhesion test results on deposited carbide coatings on beryllium oxide.

Specimen Number	Material	Thickness (μ - m)	Force (Kgm)	Tension Kgm/cm^2	Remarks
1	WC + Co dc sput	3.00	9.08	177	Substrate sheaved in cross-section
			4.20	81.7	Small piece of substrate pulled out; remaining coating adherred to substrate
2	WC dc sput	2.50	6.58	128.5	Separation at cement joint – coating well adherred to substrate
			4.20	81.7	
3	TiC RF sput	0.75	3.64	70.8	Separation at cement joint with coating particles observed in cement on pin. No interface separation
4	TiC ARE*	60.0	3.18	61.9	Coating fractured near surface with particles observed on face of pin. No interface separation

*Activated Reactive Evaporation

3.3 Task 3

Evaluation of coated bearing surfaces on operational MESG rotor and cavity parts.

Rejected rotor and cavity parts were supplied by Autonetics to aid in the development of coating processes suitable for complete and uniform coverage of the spherical bearing surfaces. Twelve rotors (part no. 12504-302) and six cavity sets consisting of six each of part no. 12678-302-1 and no. 12698-302-2 were received in May 1976 for coating as operational MESG parts. Coating was completed in March 1977 and the hardware was delivered to Autonetics for testing as directed by AFAL.

3.3.1 Rotor Coating Process

Beryllium rotor parts were coated with MoS_2 using the system shown schematically in Figure 3-25. This system uses the Sloan sputter gun with an MoS_2 target as the coating material source. Sputtering occurs when a (-) dc potential is applied to the cathode surface which in turn results in material being ejected from the cathode ID as shown by the flux lines in the diagram. The rotor is placed in a slowly rotating cup which causes it to turn during deposition.

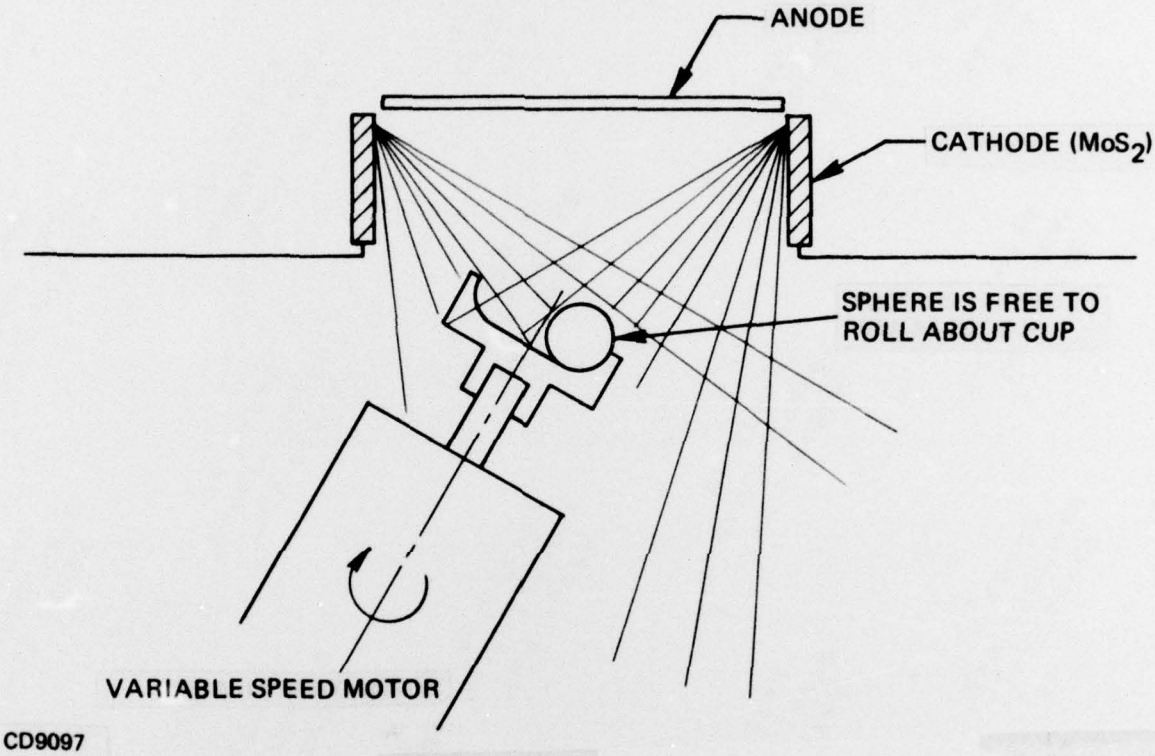

Figure 3-25. Schematic for coating spherical parts using the model S-310 dc sputter gun.

It was also found that an RF bias potential applied to the cup improved covereage of the sphere, adhesion and lubricating properties. Actual sputtering time to coat rotor parts was 15 minutes. Approximately 360 watts of power was applied to the hollow cathode target in the Sloan sputter gun and the RF bias level was 100 peak-to-peak volts on the cup and rotor part. Cleaning of the rotor prior to coating consisted of an ultra-rinse in a 60-40 mixture of distilled water and nitric acid followed by two ultrasonic rinses in distilled water and then an ultrasonic rinse in methanol followed by air drying.

3.3.2 Cavity Coating Process

The original intent was to coat cavity parts with a thick film of titanium carbide by activated reactive evaporation of titanium carbide as described in Figure 3-26 and then finish to the specified dimensional size by diamond lapping. It was found that due to the nature of the as-ground cavity surface, it was impossible to deposit a completely dense TiC coating as the coating was shown to nucleate on the individual grains composing the beryllium oxide surface. Further complications arose when it became apparent that coverage of the entire spherical surface with a coating of uniform properties could not be guaranteed. Through-hole coverage necessary for electrical connection to the bearing electrodes was also observed to be inadequate. A photomicrograph of the TiC surface after rough lapping is shown in Figure 3-27. Poor density and large voids in the coating are apparent. Coating thicknesses is approximately 50 μm.

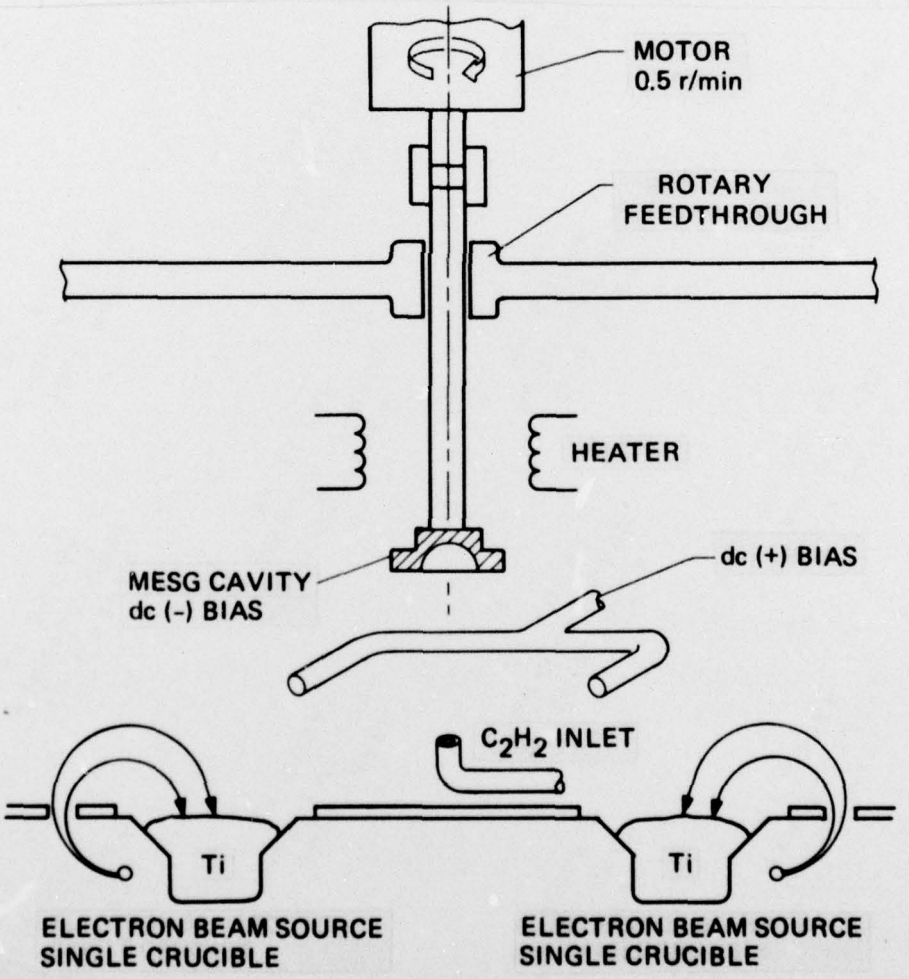

Figure 3-26. Schematic of system for the deposition of titanium carbide by activated reactive evaporation on MESG cavity parts.

3/8 GRIPPER MARGIN 1/4 TOP EDGE OF IMPRESSION PAPER 1/4 GRIPPER MARGIN 3/8

ONE INCH

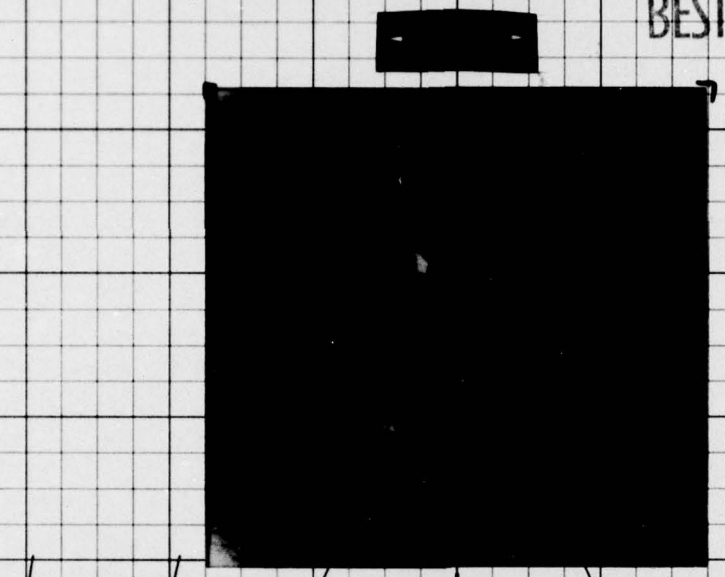

4 INCHES

3 INCHES

2 INCHES

CENTER OF

ELEVEN INCH SHEET

SIX INCHES

2 INCHES

2 INCHES

4 INCHES

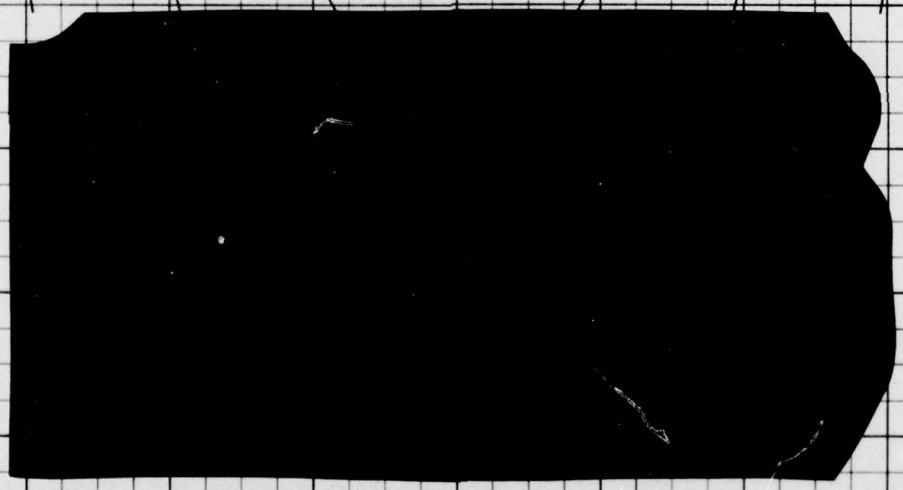

TEN INCHES

BOTTOM OF ELEVEN INCH SHEET

TWELVE INCHES

THIRTEEN INCHES

FIG. 3-27

Pg 43

IF MAXIMUM PRINTING AREA OF DUPLICATOR IS 13 INCHES LONG KEEP IMAGE ABOVE THIS LINE

GUIDE FOR RIGHT EDGE OF PLATE

GUIDE FOR RIGHT EDGE OF PLATE

DATE ORDER NO.

deposited onto the as-ground cavity surface by the combination of high rate electron beam evaporation and substrate biasing and then processed to achieve a surface for hard coating.

High rate electron beam evaporation techniques were used to deposit titanium and Inconel on beryllium oxide cavity parts as an intermediate layer to provide a lapped surface for the final WC+Co coating. Best results were obtained with parameters and ease of finish lapping. Deposition was accomplished by evaporating from two electron beam guns simultaneously with the cavity positioned and slowly rotating in the vapor field such that a uniform coating is obtained. It was also found to be necessary to put a (-) dc bias on the part for optimum density of the deposit. The common term used to describe this process is ion-plating. Coating thickness for the as-deposited layer was approximately 15.0 μm and the required time for deposition was approximately 40 minutes with 2 K-watts of power applied to each gun. Finished thickness of the intermediate layer will be approximately 4.0 μm. It was also observed that excellent through-hole coverage resulted when the negative bias was obtained. Figure 3-28 is a schematic of the system used to deposit Inconel coatings.

WC+Co coatings were then deposited onto the lapped Inconel activity surfaces using the Sloan sputter gun. Deposition was accomplished using approximately 360 watts of power applied to the cathode surface for a 60 minute time period. Prior to the WC+Co deposition, cavity parts were ultrasonically cleaned in acetone and then vacuum baked at a temperature of 200^{o}F for a minimum time period of one hour. The WC+Co surface was lapped after coating to remove any large-grain type of growths that may have protruded above the surface. The finished thickness of this film will be approximately 1.0 μm.

Grooving of the first two sets of cavity parts was accomplished by CSDL personnel using fixtures at Northrop, PPD. Some lifting of the coating was observed along the edges of the grooves indicating that modification to the grooving procedure may be necessary as the technique developed for electroless nickel coating may not be directly applicable to the harder WC+Co coatings. The remaining sets of cavity parts were delivered to Autonetics ungrooved and Autonetics has to do the grooving operation and any other required peripheral machining operations.

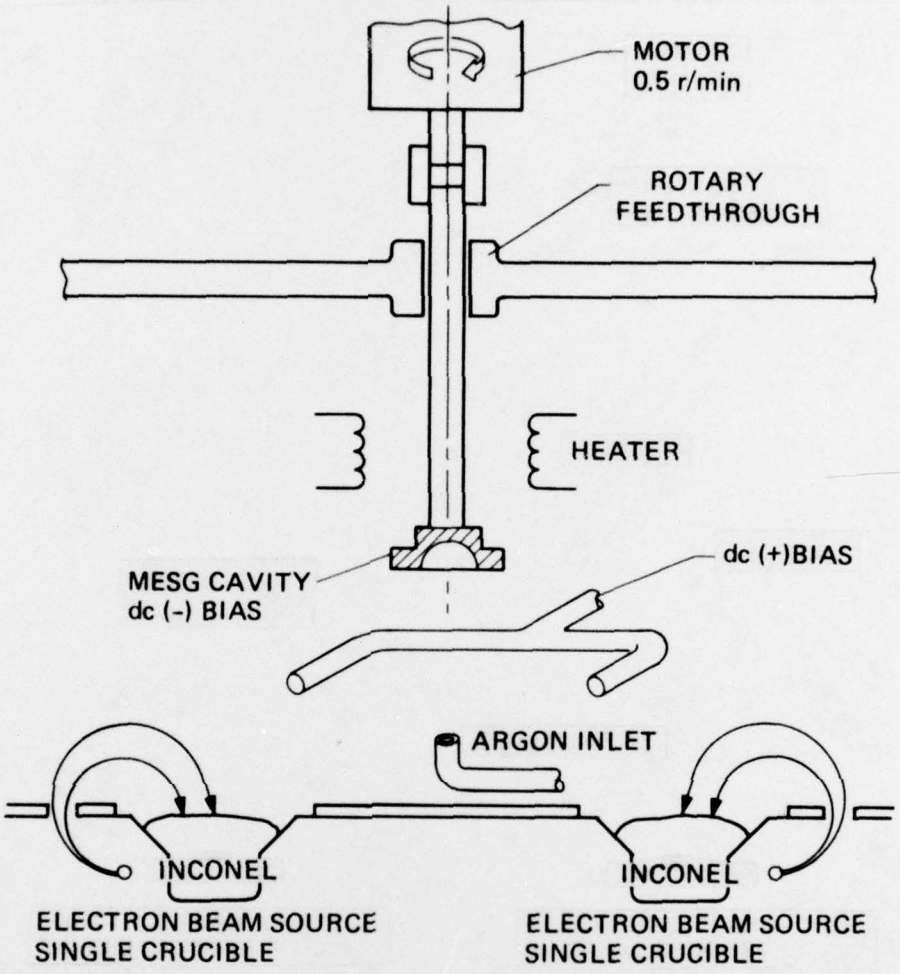

Figure 3-28. Schematic of system for the deposition of Inconel coatings on MESG parts by activated ion plating.

SECTION 4

DESIGN REVIEWS AND VISITS

18-20 February 1975:

P.R. Kerrigan of CSDL attended the Design Review held at Autcnetics and presented the current status of the CSDL nondestructible MESG program.

28 May 1975:

A program review was given to Capt. Walter Peterson and Mr. Philip Eignor of AFAL at CSDL. The purpose of the meeting was to acquaint them with the CSDL MESG program and to review the schedule for FY76 and FY77.

3 December 1975:

A visit was made by K. Taylor to Autonetics. A discussion was held with H.L. Bumps, Dr. A.L. Gross and J.B. Boltinghouse relative to coating requirements for the Micron Program.

6 April 1976:

K. Taylor visited Autonetics and discussed the results of recent tests on coatings for the MESG program.

7-9 April 1976:

K. Taylor attended the International Conference on Metallurgical Coatings in San Francisco and presented papers entitled:

"High Speed Friction and Wear Characteristics of Vapor Deposited Coatings of TiC on WC+Co in a Vacuum Environment"

"Ancillary Properties of Vapor Deposited Carbide Coatings"

31 August 1976:

K. Taylor visited with Mr. R. Riegert of Technology Materials in Santa Barbara, California for the prupose of establishing valid operating parameters for the Sloan sputtering equipment as previously described.

28 October 1976:

A program review was held at CSDL with Mr. P. Eignor of AFAL.

3 November 1976:

K. Taylor visited Northrop/PPD to discuss techniques for lapping slots in the coatings on cavity surfaces. A commitment was received from Mr. W. Merritt of Northrop/PPD to allow CSDL personnel to use the Northrop facility and fixturing to perform this operation.

1 February 1977:

K. Taylor of CSDL visited Autonetics to deliver the two sets of complete cavities and four rotors and to discuss the test procedure for these parts. Preliminary examination deemed them acceptable except for the slight spalling along the slot edges which Autonetics personnel felt will not affect performance.

Autonetics will select the best two of the four cavity parts and start the assembly operations. H.L. Bump of Autonetics felt this would take about 4 weeks.

15 February 1977:

K. Taylor and H. Singer of CSDL met with AFAL personnel to review the program. CSDL was informed that Autonetics may not be funded to continue work in the Micron Program, thus the testing of the coated parts may not be performed.

REFERENCES

1. Bunshah, R.F., U.S. Patent No. 3, 791,852. Bunshah, R.F., and A.C. Raghuram, Journal of Vacuum Science, Technology 9, 1385, 1972.

2. Buckley, D.H. and Spalvins, T., Use of Sputtering for Deposi-tioned Solid Film Lubricants, Sputtering and Ion-Plating Conference, Lewis Research Center, Cleveland, Ohio, 16 March 1972.

3. Basic Magnetic Quantities and the Measurement of the Magnetic Properties of Materials, NBS Nomograph No. 47, U.S. Department of Commerce, National Bureau of Standards.

4. Knowlton, A.E., Standard Handbook for Electrical Engineers, Eighth Edition, McGraw-Hill Book Company, Section 2-½0, 1949.

5. Maissel, L.I., and R. Glang, Handbook of Thin Film Technology, Chapter 12, Section 2, McGraw-Hill Book Company, 1970.